APPARENT SURFACE CURRENTS OVER THE MONTEREY SUBMARINE CANYON MEASURED BY THE METHOD OF TOWED ELECTRODES.

Karl Arthur Mahumed

NAVAL POSTGRADUATE SCHOOL

Monterey, California

THESIS

APPARENT SURFACE CURRENTS OVER THE
MONTEREY SUBMARINE CANYON
MEASURED BY THE METHOD OF
TOWED ELECTRODES

by

Karl Arthur Mahumed

September 1975

Thesis Advisor: R. G. Paquette

of internal waves. The observed surface currents measured with the GEK all exhibited little or no correlation with winds and tides. The flows were all generally southerly; their averages agreed with previous measurements made with the GEK. This direction of flow was opposite to the generalizations of Scott and possibly agreed with those of Pirie, depending upon the placement of one of his eddies. The k-factor for the GEK could not be determined because currents measured directly in the thermocline were found to be not correlated with the GEK measurements. However, the average current speeds were in reasonable agreement with currents measured at other times in Monterey Bay, leading to the conclusion that k cannot be much greater than the assumed value of 1.0.

Apparent Surface Currents over the Monterey Submarine Canyon Measured by the Method of Towed Electrodes

by

Karl Arthur Mahumed
Lieutenant, United States Navy
B.S., U.S. Naval Academy, 1968

Submitted in partial fulfillment of the requirements for the degree of

MASTER OF SCIENCE IN OCEANOGRAPHY

from the

NAVAL POSTGRADUATE SCHOOL

ABSTRACT

Five data cruises were taken on board R/V ACANIA to study the effect on the Geomagnetic Electrokinetograph (GEK) of various environmental factors, including winds, tides, and internal waves, over the Monterey Submarine Canyon. An *in situ* current meter was used successfully on one occasion to obtain data to establish a k-factor for the GEK in the Submarine Canyon, and to directly measure the particle velocities of internal waves. The observed surface currents measured with the GEK all exhibited little or no correlation with winds and tides. The flows were all generally southerly; their averages agreed with previous measurements made with the GEK. This direction of flow was opposite to the generalizations of Scott and possibly agreed with those of Pirie, depending upon the placement of one of his eddies. The k-factor for the GEK could not be determined because currents measured directly in the thermocline were found to be not correlated with the GEK measurements. However, the average current speeds were in reasonable agreement with currents measured at other times in Monterey Bay, leading to the conclusion that k cannot be much greater than the assumed value of 1.0.

TABLE OF CONTENTS

LIST OF TABLES

LIST OF FIGURES

ACKNOWLEDGEMENTS

There are several people who had a part in this undertaking without whose assistance nothing could have been accomplished. First and foremost, my gratitude to Dr. R. G. Paquette for initiating this thesis and for counselling, advising and when necessary, prodding me along. Woody Reynolds and the entire crew of R/V ACANIA made data collection both profitable and enjoyable; their selfless help is gratefully noted. Lt. John Hollister provided the means by which I was able to communicate with the IBM 360 and receive output. PO2 John Fanning of the Oceanography Staff assisted in on-loading and off-loading equipment, even when off duty. Last but not least, my family deserves a commendation. They were my "crew" for several cruises, and throughout the project have supported all my efforts in a manner which eased the burden of this study. To one and all, a most heartfelt thanks.

I. INTRODUCTION

A. THE PROBLEM

This study was undertaken in an attempt to examine phenomena observed twice previously during experiments with the Geomagnetic Electrokinetograph (GEK) above the Monterey Submarine Canyon. Anomalously high apparent velocities were recorded by the GEK in studies by Howton [1972] and later during a student demonstration cruise. It was believed that these high values could be the results of internal wave activity in the Canyon. Lipparelli and Beardsley [1971] postulated such an effect and computed its magnitude for frequencies as low as 1.8×10^{-4} hertz.

Howton's study had no method for detecting and recording the presence of internal waves, so no GEK-internal wave correlation could be made. The present study involved the use of the GEK, expendable bathythermograph (XBT), and an *in situ* current meter, together with wind and tide data.

Five data collection runs were taken on R/V ACANIA. The location of each run is shown in Figure 1. All five runs involved the use of the GEK and measurement of the winds and tides. Runs Two through Five involved the added use of XBT's and an *in situ* current meter, although the current meter functioned properly only once, on Run Three.

It was hoped that the same anomalous apparent values could again be observed and correlated. If the anomalies

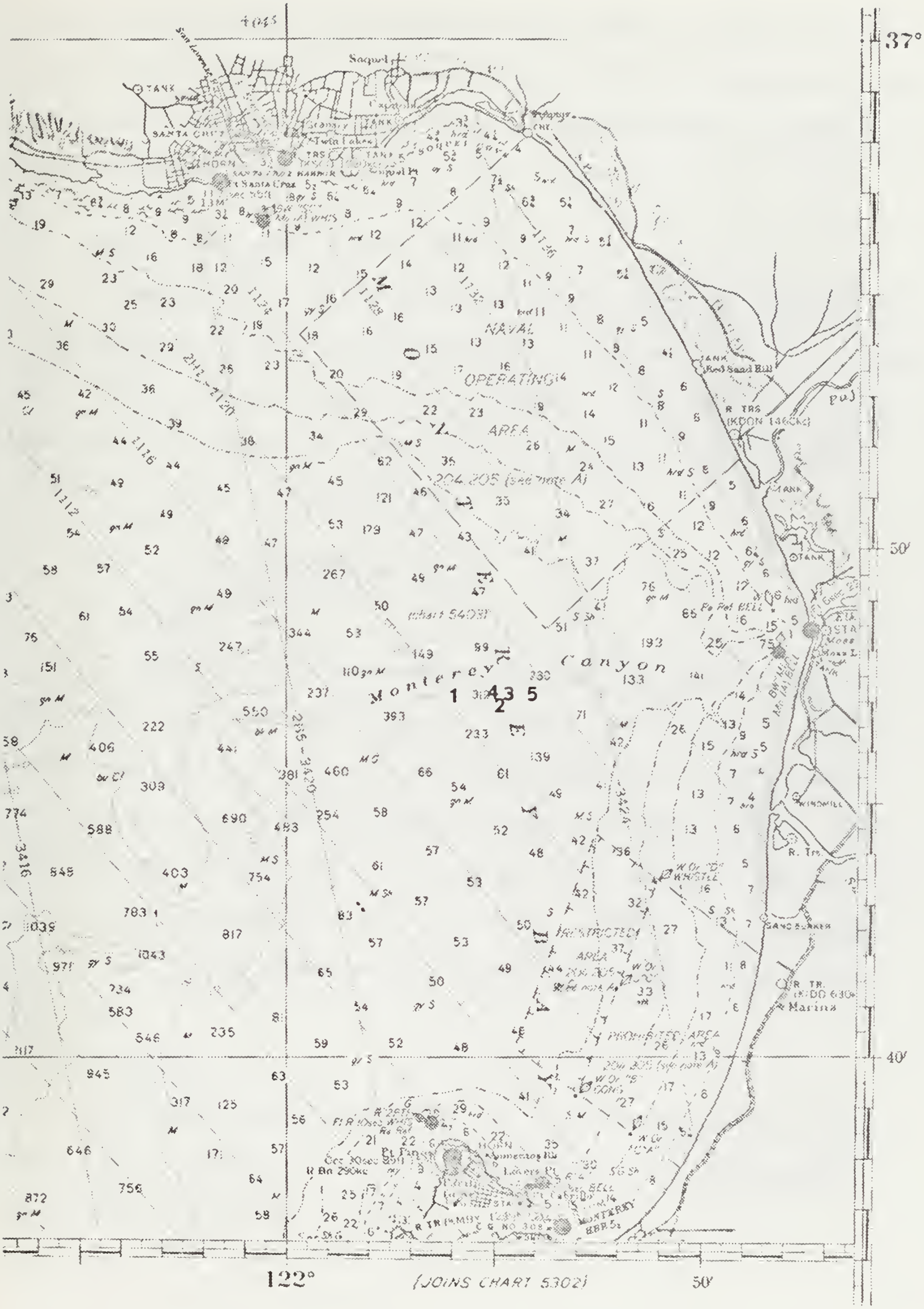

Figure 1. Area of the Present Study

were not observed, the present study hoped to widen the data base on environmental influences on surface currents over the Submarine Canyon, together with an estimate of a likely k-factor for submarine canyons.

B. USE OF THE GEK IN THIS STUDY

As employed in the present study, the GEK is capable of measuring apparent surface current velocities in the vicinity of a point, from an underway platform. Section II provides a general discussion of the theory associated with the GEK, together with its shortcomings.

C. ADDITIONAL PARAMETERS USED

1. Winds

Wind vectors were obtained from the Pacific Gas and Electric Power Station at Moss Landing, California. The anemometer is mounted on a 75-foot staff and is well away from obstructions which might perturb the wind field. The vectors are assumed to be representative of the winds in the vicinity of the data collection point. Winds were recorded hourly and are plotted as north and east components in Section IV.

2. Tides

Tides were recorded at the Naval Postgraduate School tide station and are presented, in Section IV, as heights above mean lower low water.

3. Thermocline

Thermocline depths were traced by the use of XBT drops taken periodically during Runs Two through Five. Thermocline depth and the depth of the 10°C isotherm are plotted in Section IV.

4. Geomagnetic Activity

Geomagnetic indices, A_k, were obtained from the Space Environmental Support Center, Boulder, Colorado. Values tabulated in Table I of Section II are daily averages of the geomagnetic activity as measured at Tucson, Arizona.

D. PREVIOUS STUDIES IN MONTEREY BAY

1. Stevenson [1964]

Stevenson conducted his experiment in southern Monterey Bay using drogues at three depths. He attempted to determine the wind-dependence of surface currents in the Bay. He deduced a close wind-dependence when the wind speed exceeded five knots; he found no correlation with winds and tides. Stevenson's drogues drifted to the right of the wind direction with little time lag in the rotation. He did observe one anomaly; for northwest winds, drogues drifted to the left of the wind direction.

2. Garcia [1971]

Garcia utilized totally numerical methods to model circulation in the Bay. He postulated that the major offshore currents, the California, flowing south, and the Davidson, flowing north, were the driving forces for a closed circulation system in the Bay. He noted the effect of the

Canyon in dividing the closed system into two or three dis tistinct gyres or eddies.

3. <u>McKay [1970]</u>

McKay used the GEK in studying surface currents in the vicinity of the Canyon. No attempt was made during his cruises to make a time-series measurement of currents at a point. He used a variation of cruise plan A2 from Von Arx [1950] which provides current determinations along a track, as shown in Fig. 2.

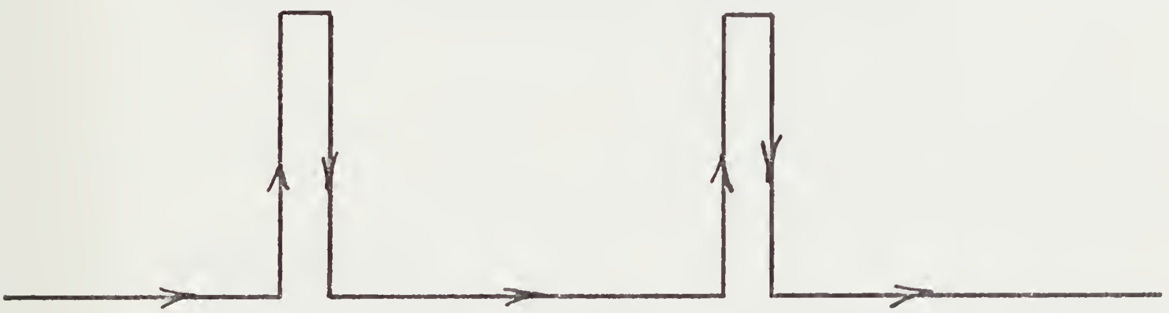

Figure 2. GEK Pattern of McKay [1970]

McKay examined the dependence of wind, sea, and tides on the apparent surface currents. He arrived at tidal dependence as the predominant result, but lacked sufficient data to adequately understand the nature of the dependence.

4. <u>Smith [1972]</u>

Smith used the GEK, together with tides and isotherm surfaces to attempt to correlate apparent surface currents above the Canyon. His cruise plan was a variation of McKay's, as shown in Fig. 3. He postulated a dynamic set of circulation

patterns but made no clear conclusion of any environmental influence on apparent surface currents.

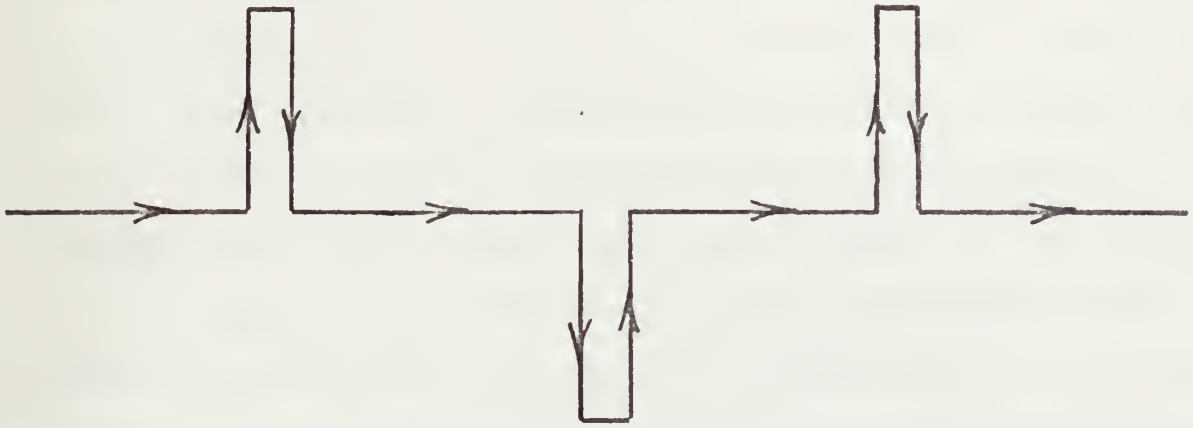

Figure 3. GEK Pattern of Smith [1972]

5. Howton [1972]

Howton used wind and tides to attempt a correlation with apparent surface currents as recorded by the GEK. He used cruise plan C-1 from Von Arx [1950], the complete traversal of a square, in order to collect time-series data at a point. He conducted six cruises at a point over the Canyon. He concluded that there are both diurnal and semi-diurnal components of the apparent surface currents which demonstrate a consistent phase relationship with the Sun and Moon. His statistical efforts showed indirect coupling of the apparent surface current with the semi-diurnal tide.

6. Pirie, et al. [1974]

In a study for the Goddard Spaceflight Center, Greenbelt, Maryland, Pirie et al. made a site study of Monterey Bay

with the emphasis placed on the applicability of remote sensors for surface current studies. His efforts were primarily to summarize all the previous work done in surface current determination in the Bay. The end product from his study is represented by generalized circulation patterns by oceanic season; Monterey Bay experiencing three climatic seasons, the Oceanic, Upwelling, and Davidson Current periods.

Figure 4 shows the generalized circulation for the Upwelling period from mid-February to late August, as proposed by Pirie et al. Four of the author's runs were taken in this period.

Figure 5 shows the generalized circulation for the Oceanic period, from September to mid-November, as proposed by Pirie et al. One of the author's runs was taken in this period.

Figure 6 is the generalized circulation in the Davidson Current period. No runs by the author were taken in this period.

Pirie concluded that the dominant driving force of the Bay's circulation is the offshore currents, with secondary influence from the wind.

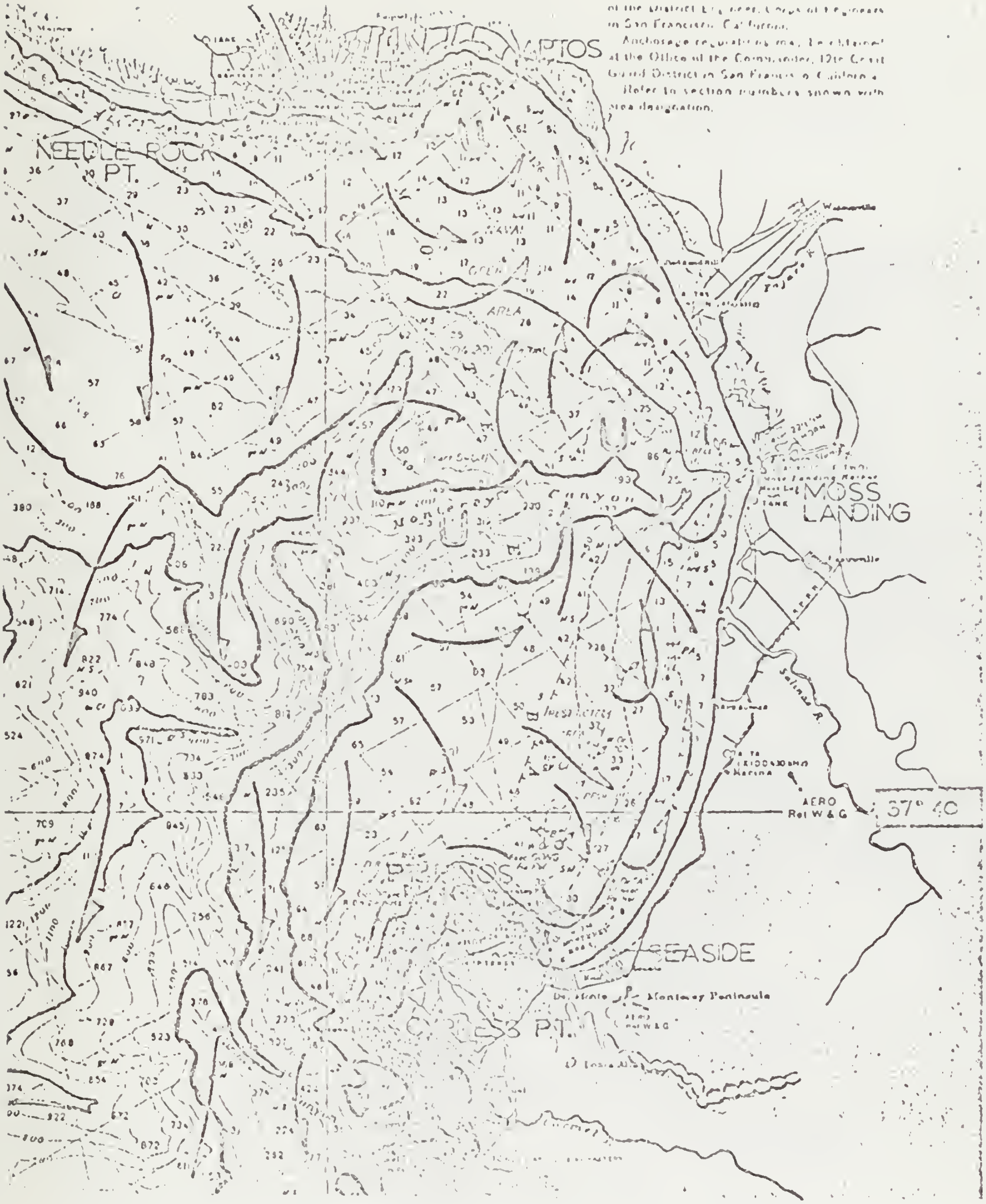

Figure 4. Generalized Upwelling Period Circulation

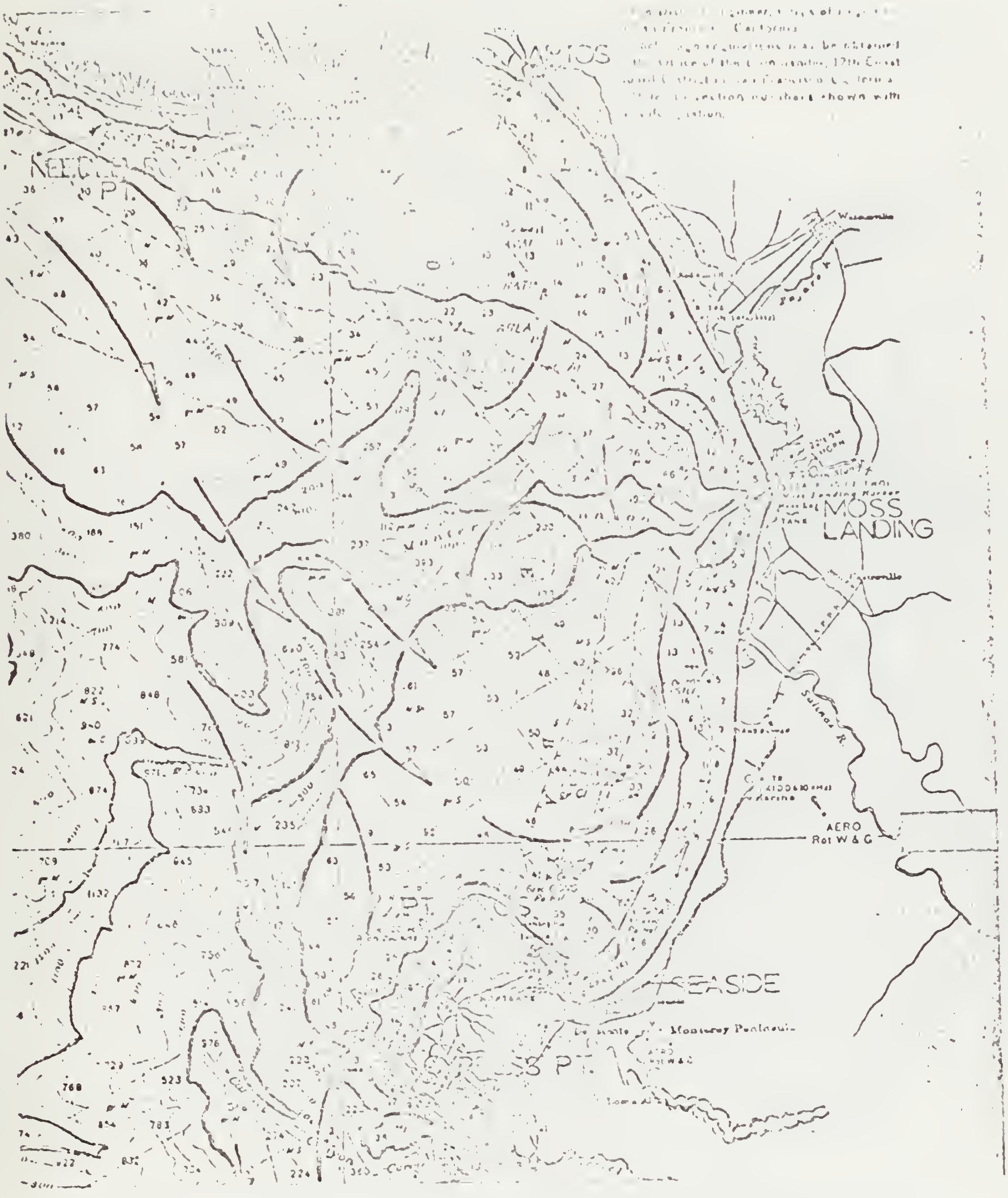

Figure 5. Generalized Oceanic Period Circulation

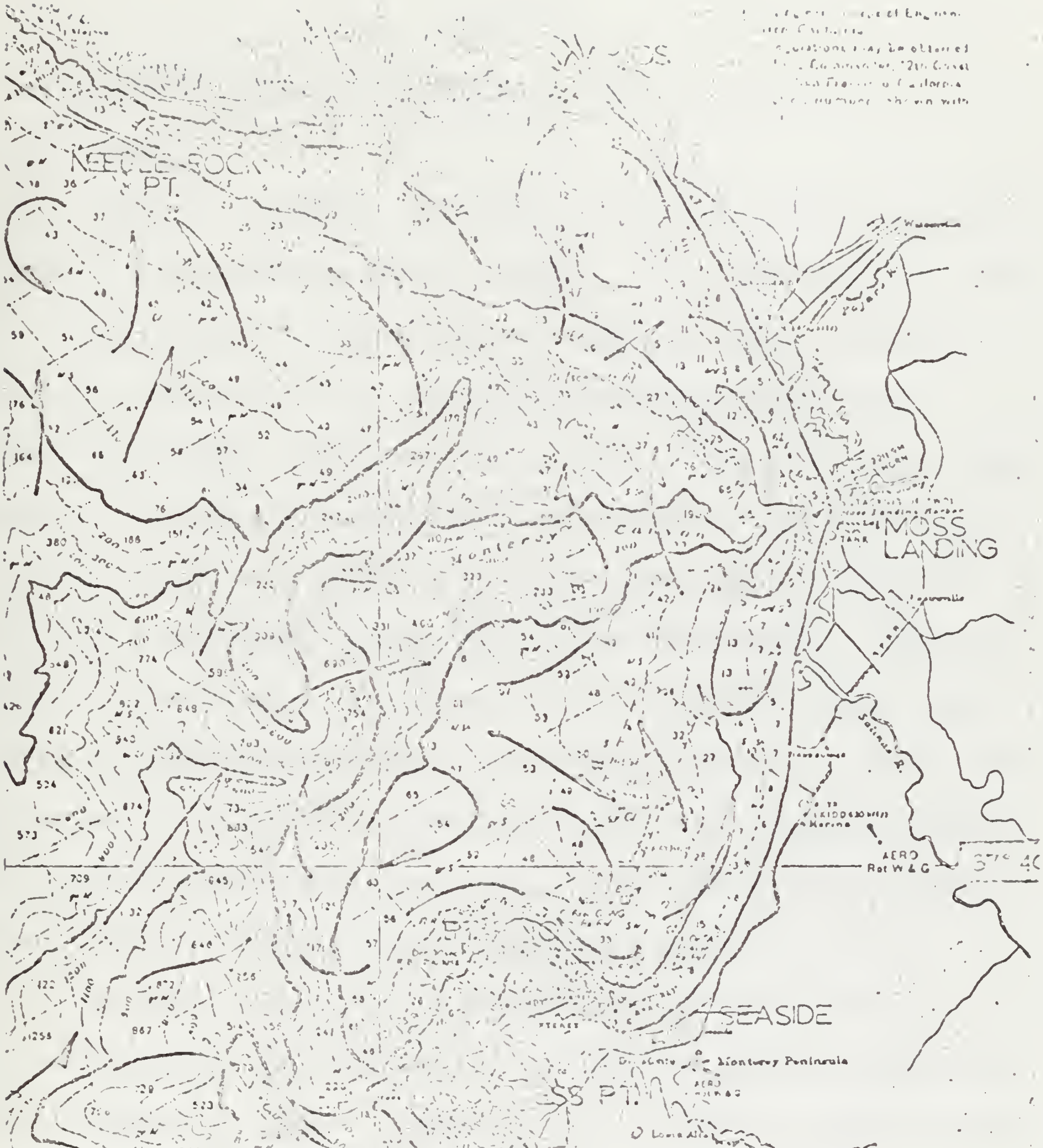

Figure 6. Generalized Davidson Current Period Circulation

II. THEORY

A. GEOMAGNETIC ELECTROKINETOGRAPH (GEK)

1. Theory

Apparent surface currents are measured by the method of towed electrodes by using the GEK. The GEK consists of a pair of non-polarized electrodes, usually silver-silver chloride, connected to a recording potentiometer by a neutrally-buoyant, two-conductor cable. The electrodes are normally 100 meters apart, each connected to an individual conductor. The use of neutrally-buoyant cable eliminates any cable droop which might degrade measurements. The electrodes must be towed far enough astern of the towing ship to be free of ship-induced electromagnetic effects (usually two to three ship lengths). Von Arx [1950] and Longuet-Higgins, Stern and Stommel [1954] are the sources of detailed description and derivation of towed-electrode theory.

Faraday, in 1832, proposed the induction of an electro-magnetic force (e.m.f.) in water moving through the earth's magnetic field. Equation (1) permits a quantitative calculation of this e.m.f., E.

$$E = vxH_z \times 10^{-8} \text{ volt} \qquad (1)$$

E = induced e.m.f. (directed perpendicular to current vector)

v = horizontal current velocity (cm/sec)

x = distance over which v is measured (cm)

H_z = vertical component of earth's magnetic field (gauss).

If the water everywhere is not moving at the same velocity, electrical currents will flow because of the potential differences. The generated potentials are decreased by the resistive potential difference due to the current flow. Generally, a space integral of $E - ir$ is required to find the potential field and the distribution of current density, i, given the resistivity, r.

Ideally, the velocity maximum is at the surface, and there exists beneath this surface layer a thick layer of essentially static water, which acts as a low-resistance shunt upon the resistive voltage generators near the surface, bringing the potential gradient to near zero. If then, two identical electrodes are towed through the water, they themselves are at equal potential. But the single length of wire between the electrodes is being carried transversely through the vertical components of the Earth's magnetic field by the athwartship component of the surface current, which affects both cable and ship. The voltage recorded aboard the ship then is generated in this wire according to equation (1). A thick, conductive bottom could serve the same purpose as a static water layer.

If there is not a static layer below the surface layer and the bottom is more or less insulating, the voltage in the sea between the electrodes will not be zero and the signal due to the surface currents will be altered. If the current were the same at all depths, no voltage would be measured. If there were a reversed rapid flow near the

bottom, the voltage at the surface might be augmented. If rapid flow was present at mid-depth and the cross-section of the static conducting path were not great enough to dissipate it, its influence would be felt at the surface. Thus, surges and internal waves can affect the voltage measured by the GEK if the particle motion reaches the surface. The effect may still be felt if the water is not too deep, if the motions extend to near the bottom, or if the motion does not reach the surface. The resulting anomaly may either add to or subtract from the signal otherwise present at the surface, depending upon the relative direction of the flow.

The precise calculation of the effects of such a phenomenon presents considerable difficulty involving three-dimensional integration (probably by numerical methods) and requiring a knowledge of the water velocity at all points in the volume. For this reason, the treatment of the phenomenon in this study is only semi-quantitative.

Since Monterey Canyon is of moderate depth, it was anticipated that it might approximate an ideal case when surges are absent and that the degeneration which results in the necessity of raising the k-factor to above unity is fairly small. Part of the objectives of this study was to test this hypothesis by comparing the GEK-measured surface currents with directly measured currents. However, as will be seen, a current meter in the thermocline exhibited little correlation with currents at the surface.

2. Errors

There are several sources of significant errors in the measurement of apparent surface currents by the GEK:

a. Deep currents or the effects of depth which result in a k-factor change, as discussed above. This results in an error in magnitude only, if the degeneration is an effect of an insufficient static layer. The sides of the canyon may also distort the electric field.

b. Geomagnetic disturbances can disrupt the Earth's magnetic field. According to Longuet-Higgins, Stern, and Stommel, variations equivalent to 0.1 knot can be expected over long-term measurements, with maximum errors of 5 knots possible during major solar storms. Bennett and Filloux [1975], in a month of data collected in the deep Atlantic, rarely observed electrical fields in excess of 0.25 mv/100 m, equivalent to 0.13 knot; apparently Longuet-Higgins' 5-knot variations are not realistic, at least in deep water.

Table I lists the geomagnetic activity for the days on which data was collected. It will be seen that the stormy conditions of 11 November 1974 coincide with the GEK records for that date, and may account for the observed high apparent values at that time.

TABLE I

Geomagnetic Activity

Run	Date	Geomagnetic Index	Condition
1	10 Nov 74	6	Quiet
	11 Nov 74	31	Minor Storm
2	26 Feb 75	6	Quiet
	27 Feb 75	5	Quiet
3	3 Apr 75	5	Quiet
	4 Apr 75	5	Quiet
4	21 Apr 75	12	Unsettled
	22 Apr 75	13	Unsettled
5	1 May 75	6	Quiet
	2 May 75	15	Active

c. Zero-point drift of the electrodes can result in errors. This drift can be the result of electrode deterioration or cable leaks. Drifts in the present study were either controlled or were slow enough to be negligible.

d. It should be noted that over the submarine canyon Howton found the currents on opposite sides of his square significantly different so that the zero derived by comparing tows on reciprocal courses has an element of uncertainty. This error was minimized in this study by using the L-shaped tow pattern in which the reciprocal courses are close together in both time and space. Section III discusses the tow plan.

B. INTERNAL WAVES

We will first consider a simple, two-layer system, as shown in Fig. 7. In this system, internal waves are those waves within the water mass and on the interfacial boundary.

If the wave shown is progressive, from left to right, particles in the cell A-B-C will orbit in a clockwise manner while particles in the C-D-E cell will orbit in a counter-clockwise manner.

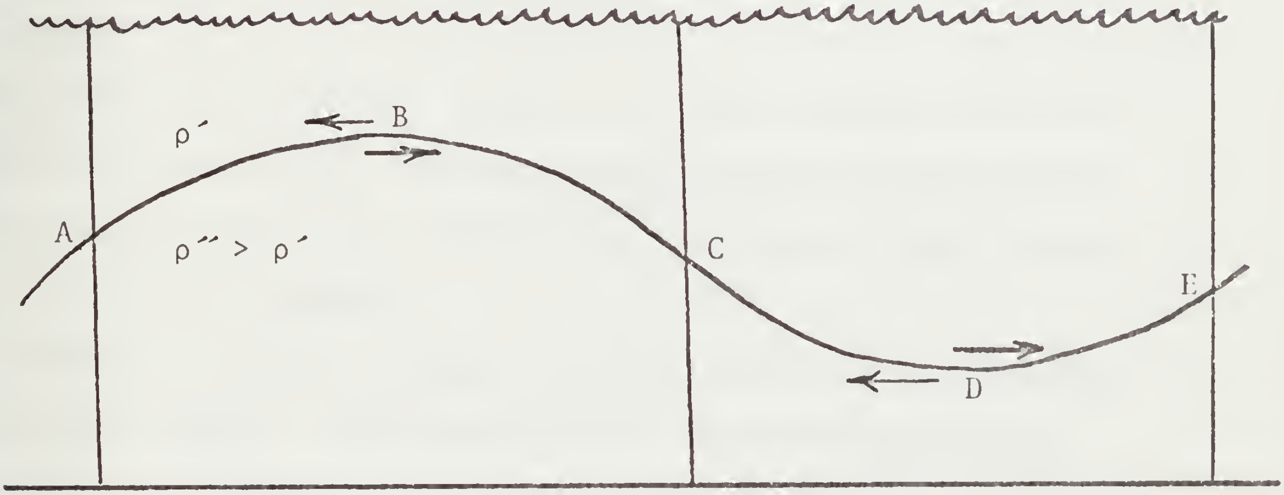

Figure 7. Simple Internal Wave

If the apparent surface current is also moving from left to right, it can be seen that the apparent surface current will alternately experience degradation and enhancement as the internal wave progresses past the point of measurement. Motions in the lower layer also will contribute to the potentials measured.

These simple internal waves are the only ones possible in the two-layer model discussed above. The ocean is not two-layered, and there are an infinite number of possible internal waves which can occur in the continuous density gradients in a given water mass anywhere in the ocean.

Since the tidal character of internal waves is so prominent, tides were for some time considered to be the only cause of internal waves by forcing a tidal oscillation of the density boundary, either near shore or in deep water.

Internal waves need not be clearly periodic. Aperiodic characteristics, such as wind-induced surges, are also possible. The effect of an onshore wind into a semi-enclosed basin can cause these aperiodic internal waves by building up surface water at the coastline, depressing the boundary, and setting the boundary in motion.

There is reason to expect internal waves in the Monterey Submarine Canyon. McClelland [1972] obtained fragmentary records of internal waves in the Canyon. He noted a 90-meter movement of the 7°C isotherm in a period of 3 hours. Motion of that order was not seen in any of the data for the present study; most of the internal waves observed were of the order of 20-30 meters.

Shepard [1974] observed internal waves in the Canyon to be moving up-canyon at speeds of 25-88 cm/sec. In other experiments off San Diego, Shepard observed the passage of the same internal wave over the shelf and in a canyon. His results showed that the canyon-confined wave propagated faster than the wave over the shelf, suggesting that the constriction of the canyon walls tends to increase propagation speed.

The work of Lipparelli [1971] suggested that the effects of internal waves on the GEK might be important. He computed the effect of short-period, idealized, free internal waves on

GEK signals. He modelled a two-layer ocean and limited his study to free internal waves which would form on the interface. The concern in the present study is with a wave forced at semi-diurnal frequency and with a wave number of $10^{-4}\,m^{-1}$. Extrapolation of Lipparelli's results to such wave numbers and to a 12.4 hour period for depths and densities appropriate to the canyon yields a signal of about 10 mv/100 m, corresponding to 5 knots. This must be regarded as an order of magnitude only, since the canyon is far more complex than Lipparelli's model. The calculations do suggest that sizeable effects of internal waves may be expected.

The length of time-series was limited by practical considerations to periods of a little less than 24 hours (see Section III for details). With this length of series, it would be possible to extract a 12.4 hour periodic component reliably only if the data were relatively free of other frequencies and noise. As will be seen, this latter property did not prevail and neither tidal components nor any other characteristic period could be extracted with certainty.

III. PROCEDURE

A. CRUISE PLAN

Sailing plan C-2 from Von Arx [1950] was chosen for this study (see Figure 8). The dogleg plan has advantages over the previously discussed square plan used by Howton [1972]. Howton's fixes were obtained by summing reciprocal courses on opposite sides of the square. The sum resulted in a zero-point for that pair of courses and the apparent velocity perpendicular to that course could then be determined as the difference to the right or left of a zero-point. One circuit of the square resulted in two pairs of two differences. Using successive vector sums, apparent current velocity could be calculated twice per circuit of the square.

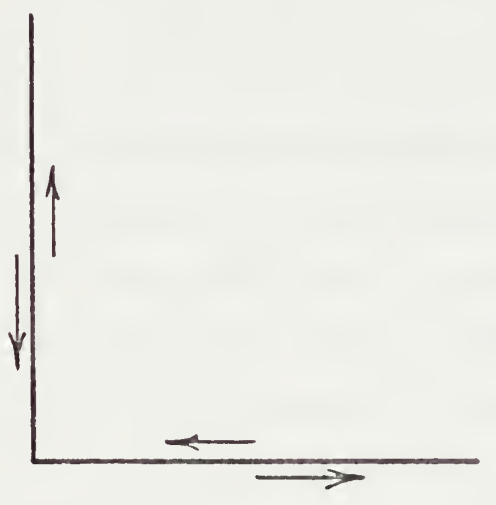

Figure 8. GEK Pattern

The dogleg plan used in the present study essentially "folds" the square in half diagonally. This results in reciprocal courses being transited on (ideally) the same track. Howton's reciprocals were separated by the width of the sailing plan. Fixes for the present study were calculated in the same manner as Howton, by using a leapfrog scheme wherein each value of apparent current is used for two separate calculations. Table II shows the sequence of obtaining a fix.

TABLE II

Fix Determination

Fix No.	Track Segment E/S	Track Segment N/S
1	$A_1 - B_1$	$B_1 - C_1$
2	$B_2 - A_2$	$C_1 - B_2$
3	$A_2 - B_3$	$B_3 - C_2$
4	$B_4 - A_3$	$C_2 - B_4$

At a speed of six knots, a complete traversal of the track took about forty minutes, so a fix was obtained about every twenty minutes. At each end of the track, Williamson turns were executed to maintain the proper track. Occasional variation of the track was necessitated by fishing boats, fishing buoys, or mechanical problems of the ship. During these deviations from the track, no data was recorded until the track had been reestablished. With the exception of a two hour break in the data for Run Three, no data gaps exceeded thirty minutes.

It had originally been planned to make all data collection in 24-hour periods, but ship commitments or equipment malfunctions prevented this. Table III lists run durations.

TABLE III

Run Duration

Run No.	Duration (hrs)
1	20
2	23.5
3	19.5
4	20.5
5	21

Although no cruises lasted as long as had been planned, lengths of records were long enough to give a reasonable probability of encountering anomalous events and correlating between tides, winds, and directly-measured currents, provided such correlations were strong.

Program KAMGEEK, Figure A-1, was used to calculate the apparent current vectors. The program computed resultant vectors from the north and east components read from the strip chart of the recording potentiometer.

B. CURRENT METER EMPLOYMENT

The Hydro Products Model 502 current meter was used as the *in situ* meter for Runs Two through Five. However, the meter worked properly only on Run Three. Data was read at fifteen minute intervals from the strip chart output of the current meter for reduction; the components are listed in Table A-VI.

Figure 9 shows the anchoring scheme used for the current meter. The subsurface float was intended to support the array vertically with 150 pounds net buoyancy. The surface float, also of 150 pounds net buoyancy, the spar buoy, of 100 pounds buoyancy, and the surface marker were intended to provide about 200 percent of the total array weight in buoyancy in order to prevent the array from sinking should the anchor slip into deeper water. One-half inch braided nylon was used to connect the current meter to the anchor: three-eighths inch polypropylene line was used for the remainder of the array.

The array was deployed in reverse order; marker, surface float, subsurface float, current meter, and anchor line. Once the proper position had been reached, the anchor was released, and the array sank. After it had been determined that the anchor was stationary, the spar buoy, with strobe lights and radar reflector, was attached to the marker. The position of the array was then established as Point B in the cruise plan.

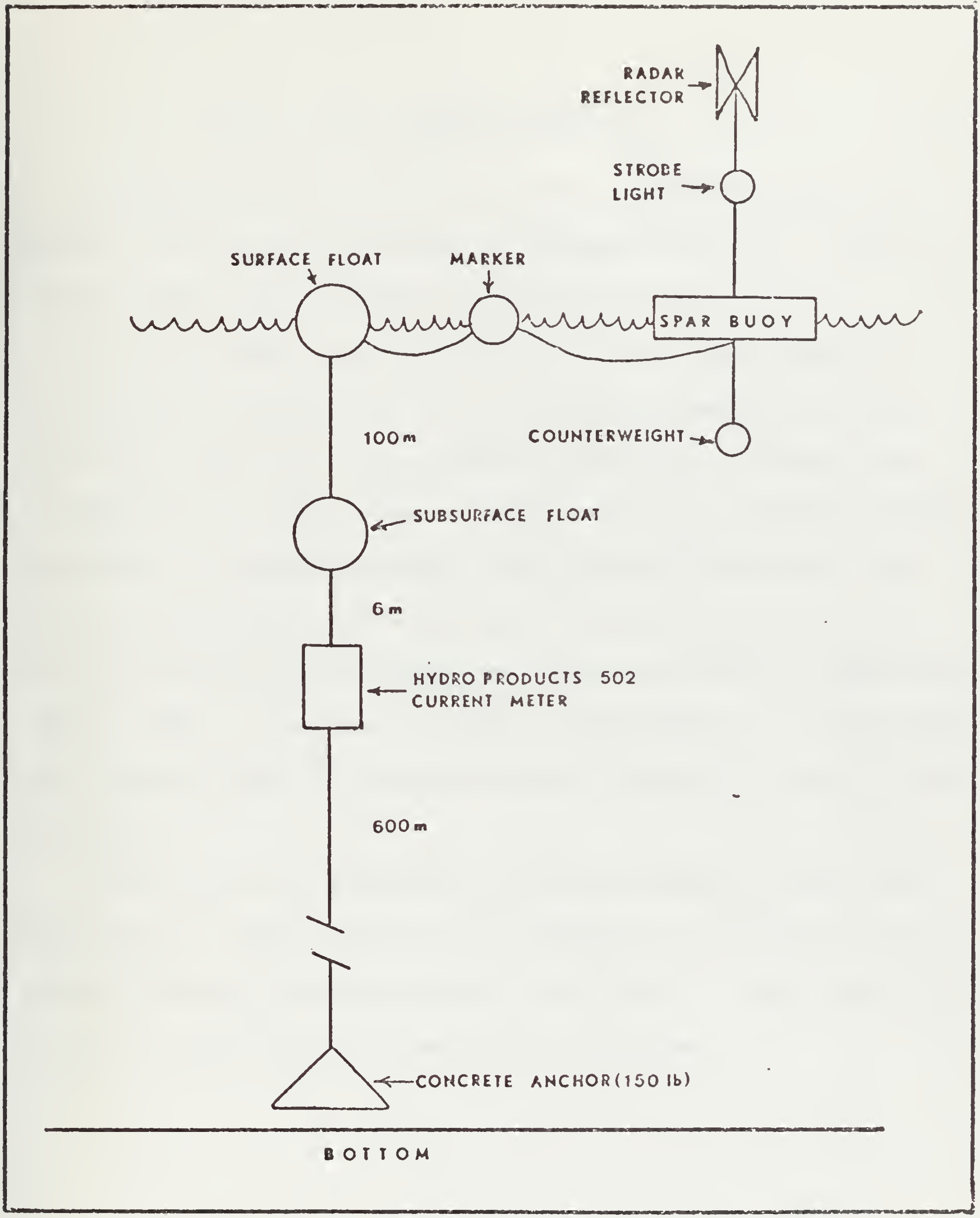

Figure 9. Current Meter Anchoring

IV. CRUISE SYNOPSES

The data are presented in several different graphical forms in Figures 10 through 31, grouped by runs. The different forms of presentation are discussed below.

For each data collection run, GEK and wind data are graphically presented in north and east components versus time; the tide height and depth of the 10°C isotherm and thermocline are also shown. Wind speeds are divided by 10 relative to the speed scale. The current meter data are added in Run Three and they have been multiplied by 5 in order to provide resolution in the north-setting components (Figure 18). In order to permit comparison of the GEK and the current meter on the same scale, Figures 20 and 21 are included.

Vector scatter diagrams were drawn manually from GEK components. Progressive vector diagrams were drawn using the VECTORDRAW program of Hollister [1975]. Note that the scales are different on individual diagrams.

A. RUN ONE

Date: 1200, 10 November 1974 - 1200, 11 November 1974

Coordinates:

A- 36° - 46.7'N, 121° - 54.9'W

B- 36° - 46.7'N, 121° - 56.0'W

C- 36° - 47.5'N, 121° - 56.0'W

65 Data Points

Vector Average: 9.39 cm/sec @ 152.5°T

Note: No temperature data was available for this run due to the lack of XBT's on R/V ACANIA.

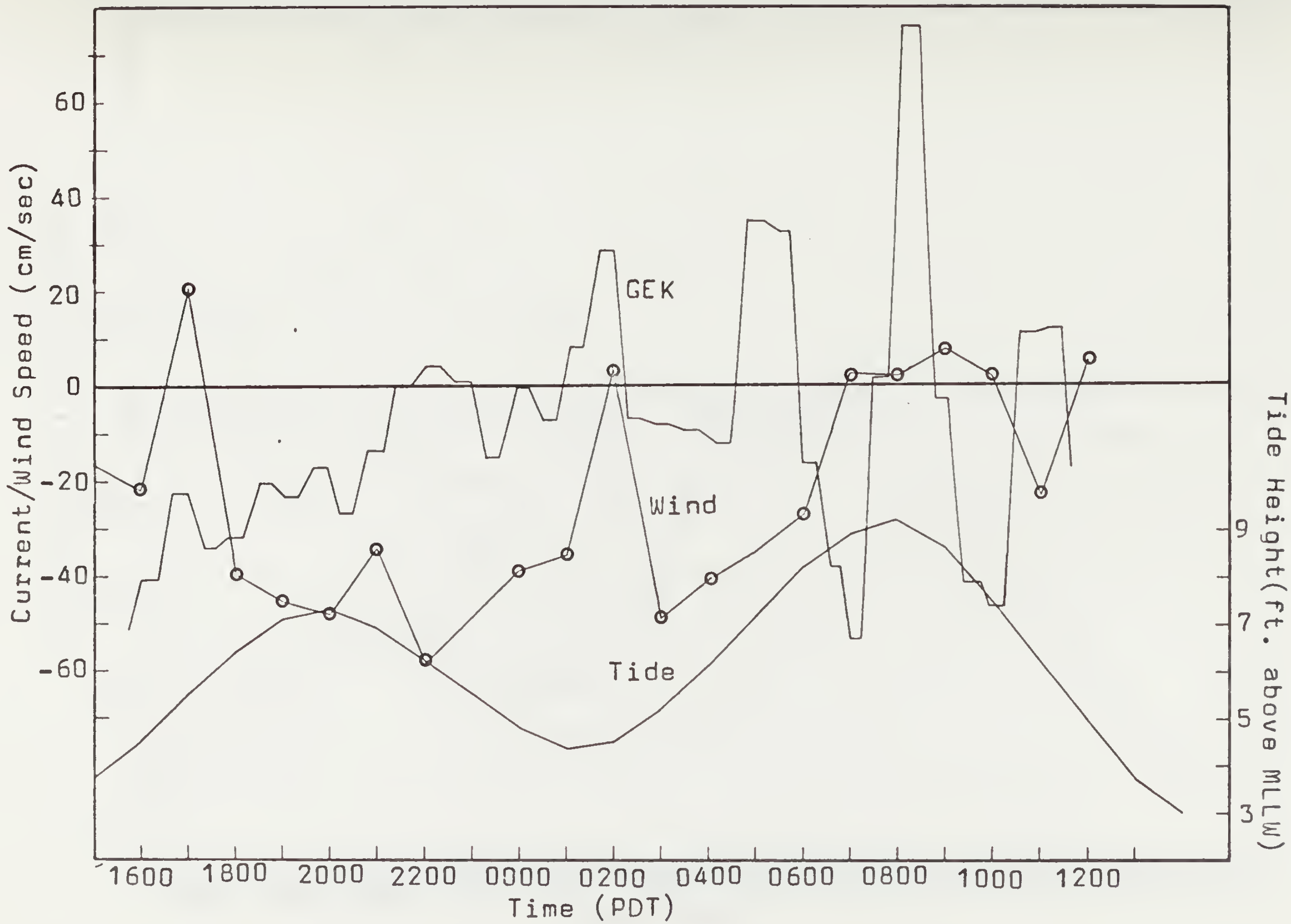

Figure 10. Run 1, North-Setting Components of GEK and Wind, Tide Height. For wind speed, read 10 times scale reading.

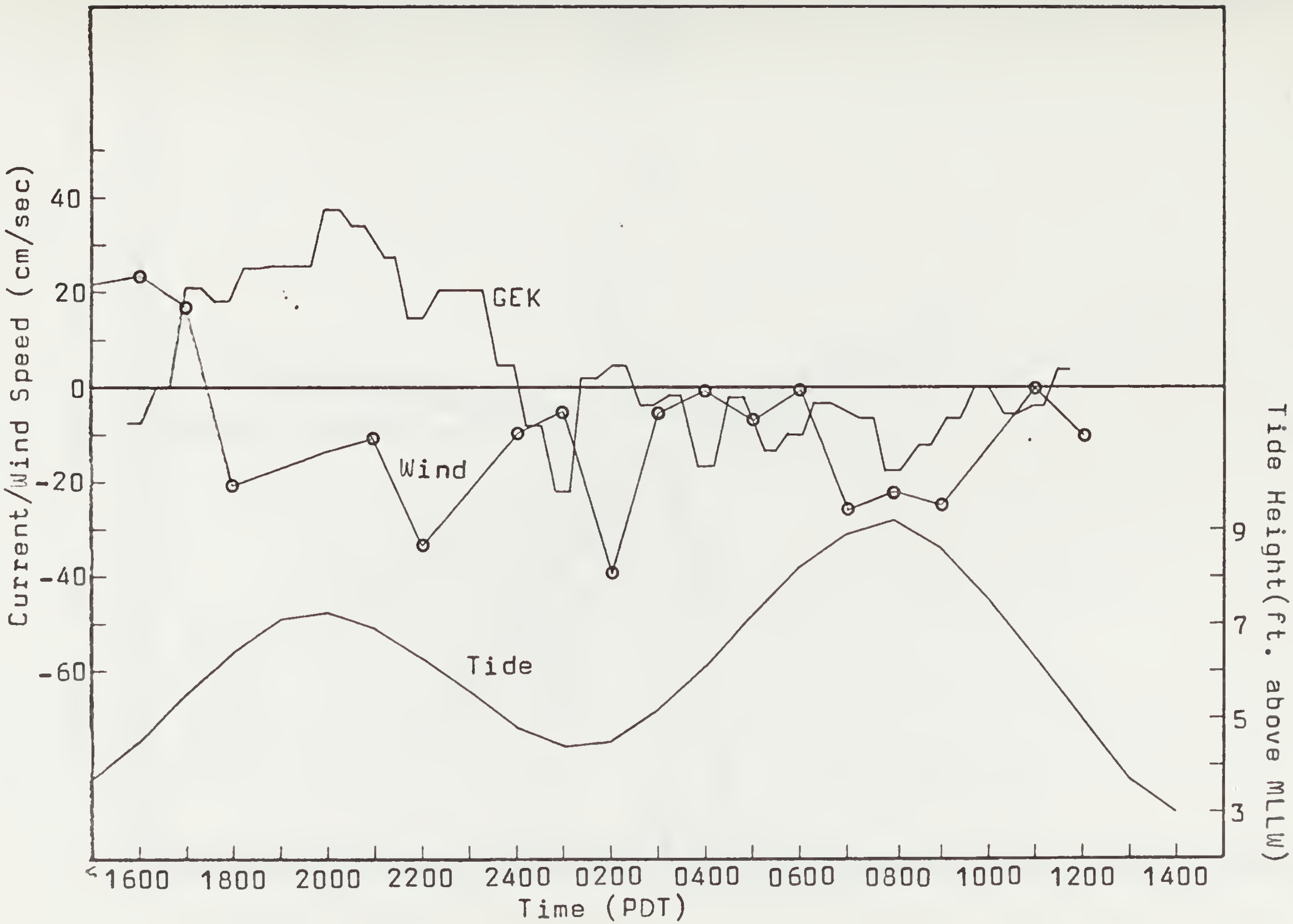

Figure 11. Run 1, East-Setting Components of GEK and Wind, Tide Height. For wind speed, read 10 times scale reading.

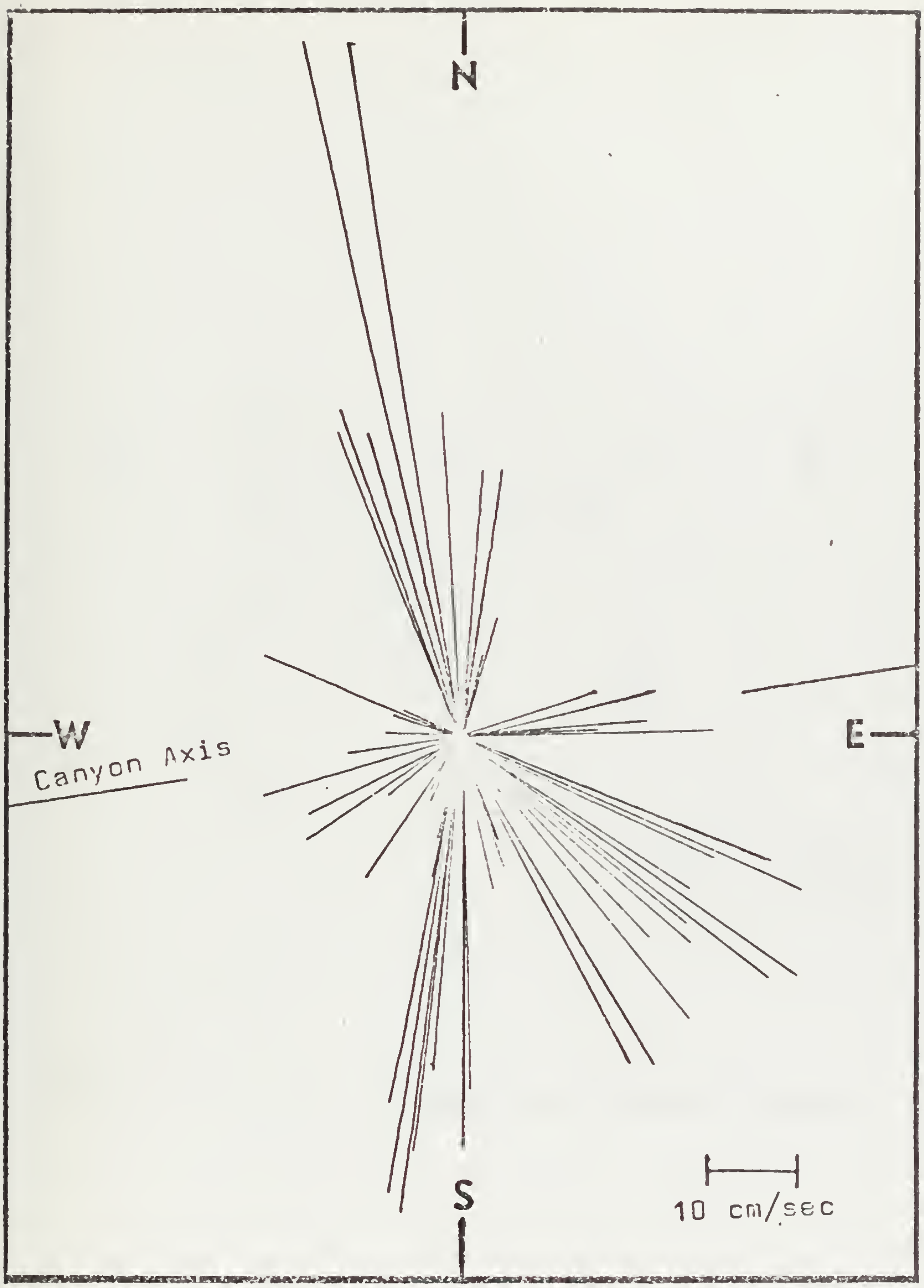

Figure 12. Run 1, Vector Scatter Diagram

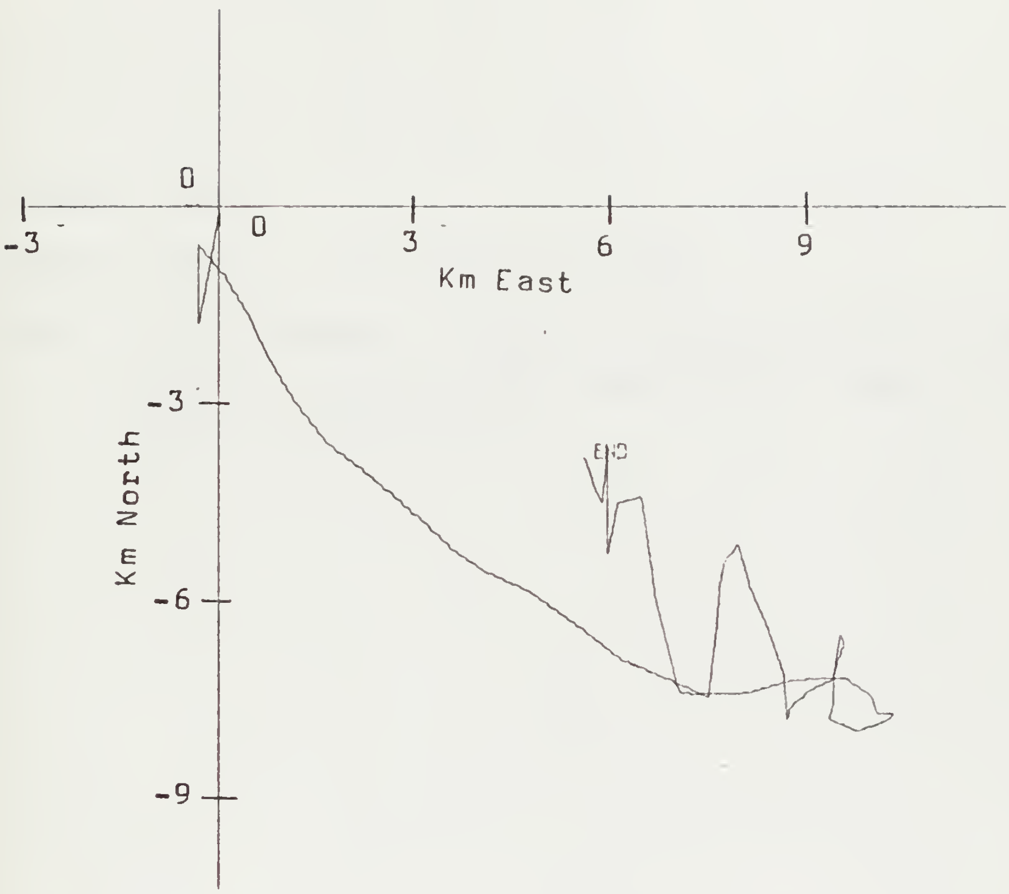

Figure 13. Run 1, Progressive Vector Diagram

B. RUN TWO

Date: 1000, 26 February 1975 - 0900, 27 February 1975

Coordinates:

A- 36° - 46.9'N, 121° - 53.9'W

B- 36° - 46.9'N, 121° - 54.9'W

C- 36° - 47.75'N, 121° - 54.9'W

49 Data Points

Vector Average: 7.47 cm/sec @ 226°T

Note: The low number of data points was due to a slower speed on this run made necessary by loss of one engine on R/V ACANIA.

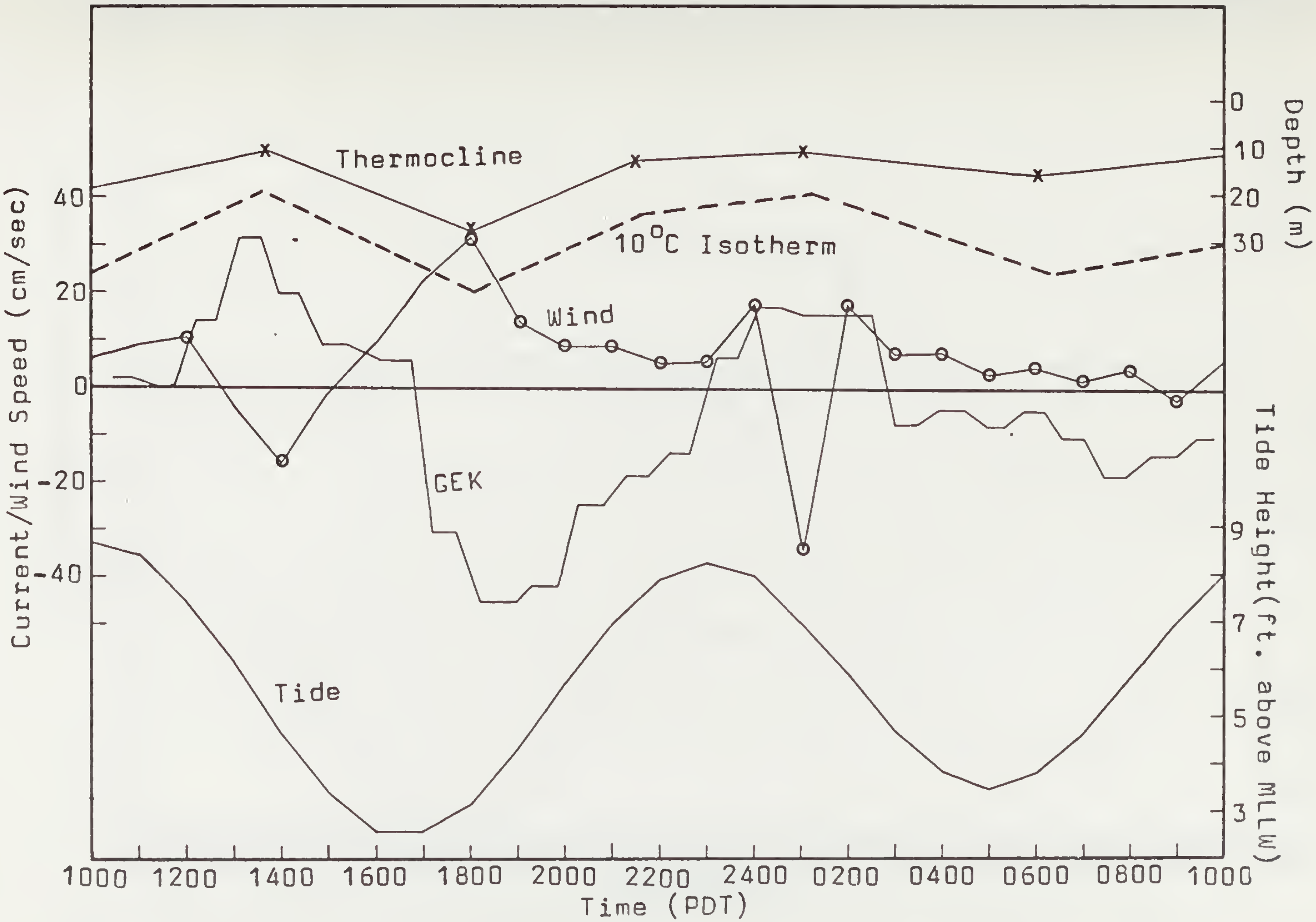

Figure 14. Run 2, North-Setting Components of GEK and Wind, Tide Height, and Depth of Thermocline and 10°C Isotherm. For wind speed, read 10 times scale reading.

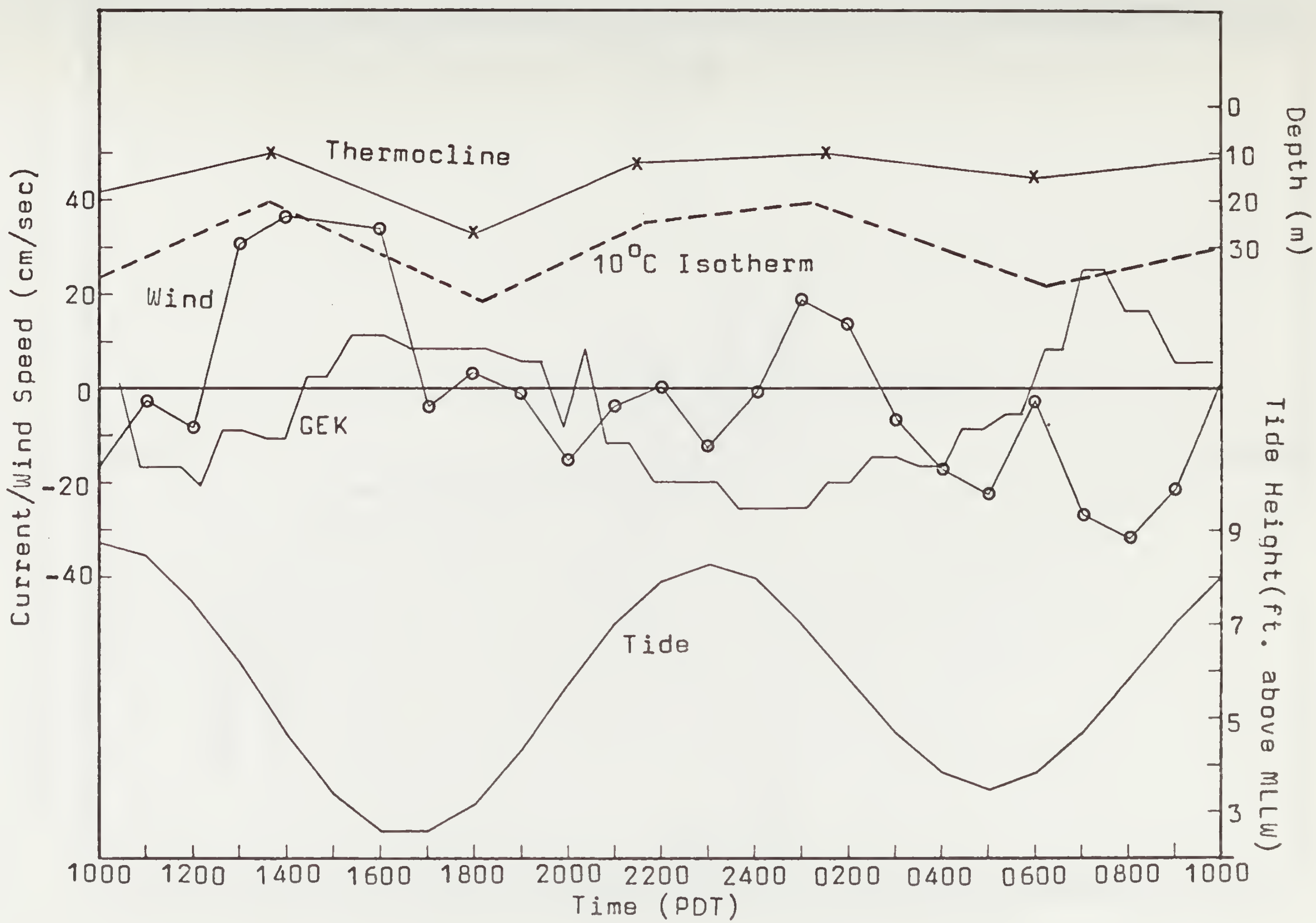

Figure 15. Run 2, East-Setting Components of GEK and Wind, Tide Height, and Depth of Thermocline and 10°C Isotherm. For wind speed, read 10 times scale reading.

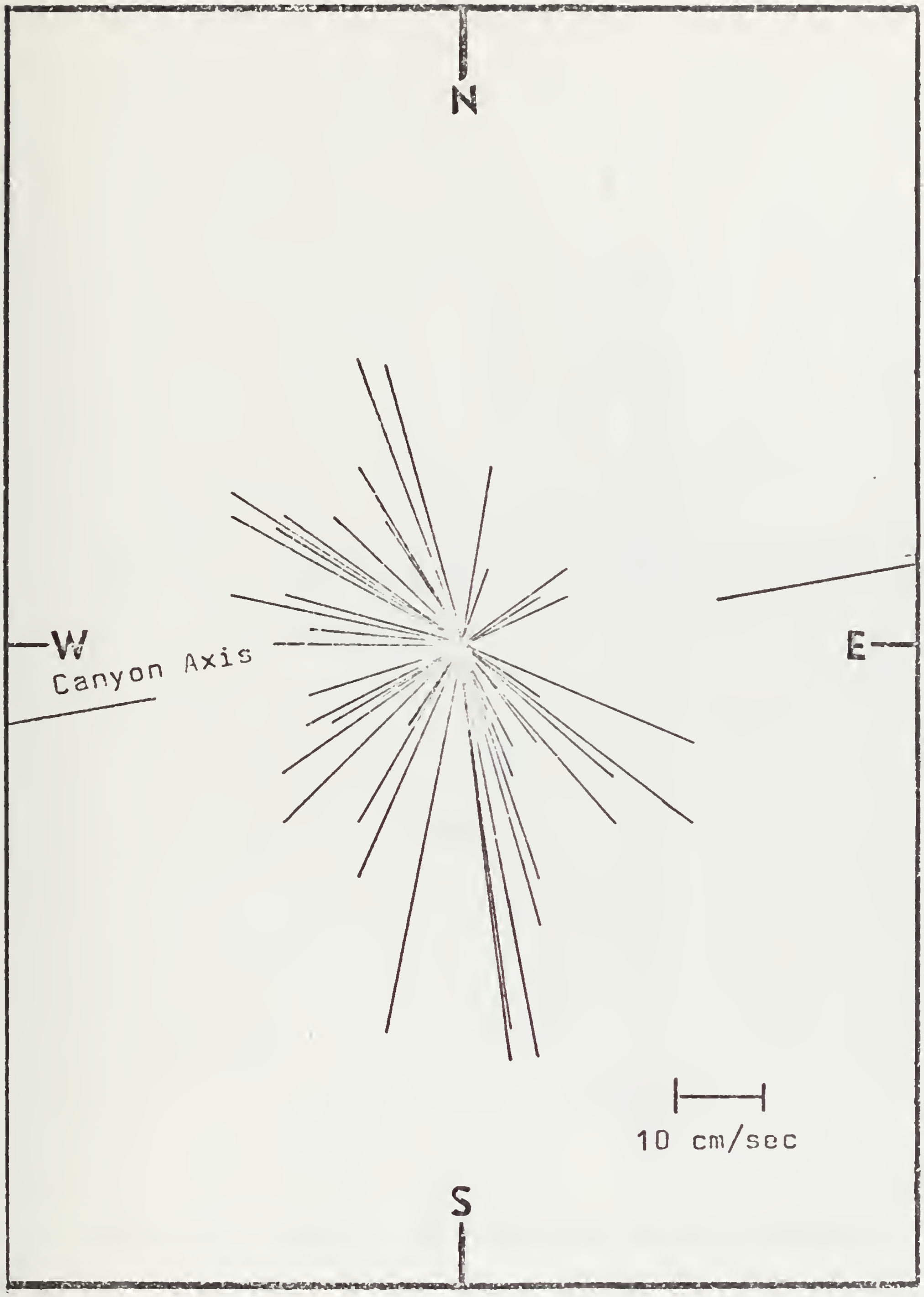

Figure 16. Run 2, Vector Scatter Diagram

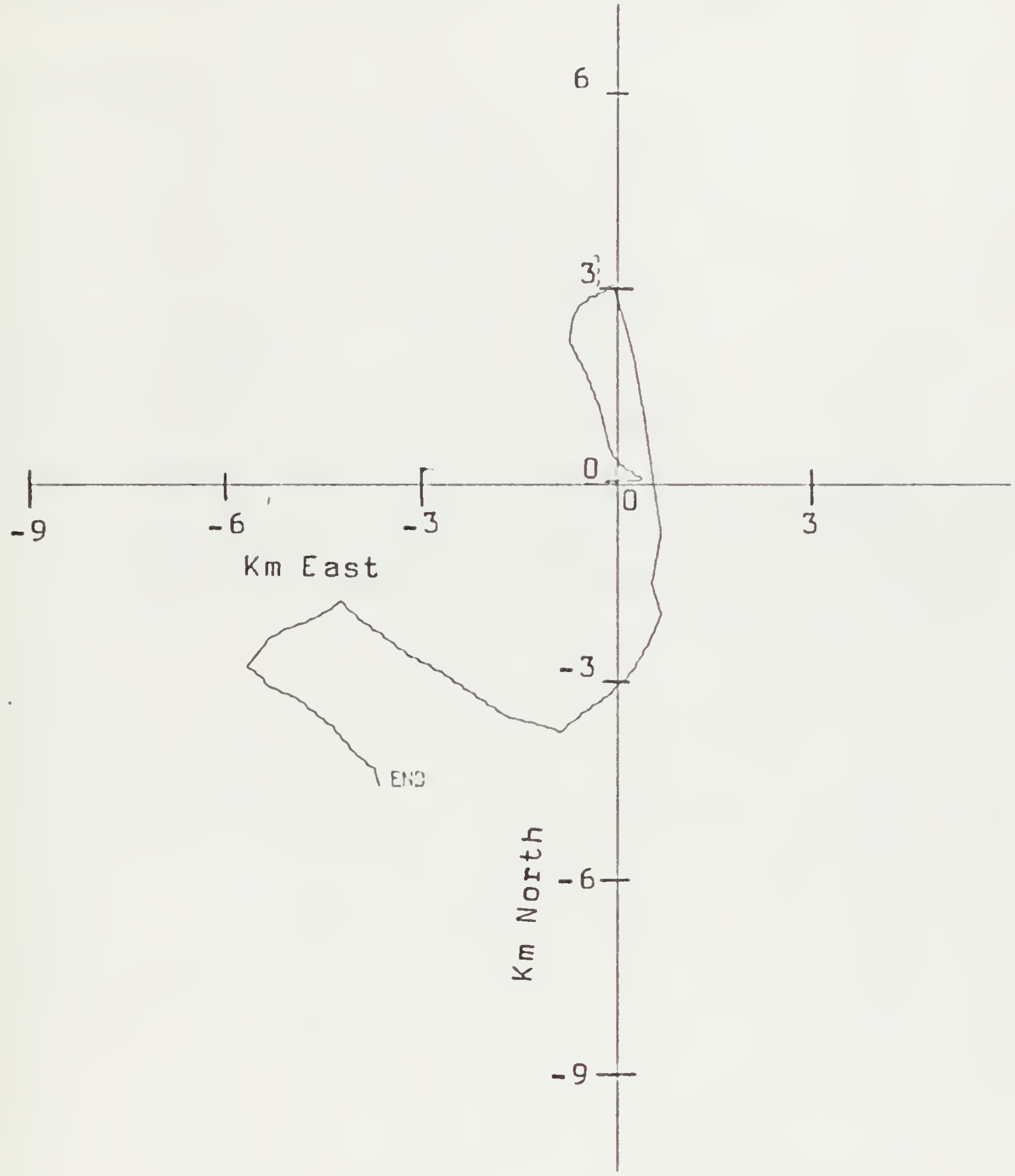

Figure 17. Run 2, Progressive Vector Diagram

C. RUN THREE

Date: 1000, 3 April 1975 - 0900, 4 April 1975

Coordinates:

A- 36° - 47.0'N, 121° - 53.75'W

B- 36° - 47.0'N, 121° - 54.7'W

C- 36° - 47.75'N, 121° - 54.7'W

58 Data Points

Vector Average: .69 cm/sec @ 180°T

Note: During this run the cable and electrodes had to be reeled in to resolder a leaking electrode. This resulted in a two-hour gap in the data.

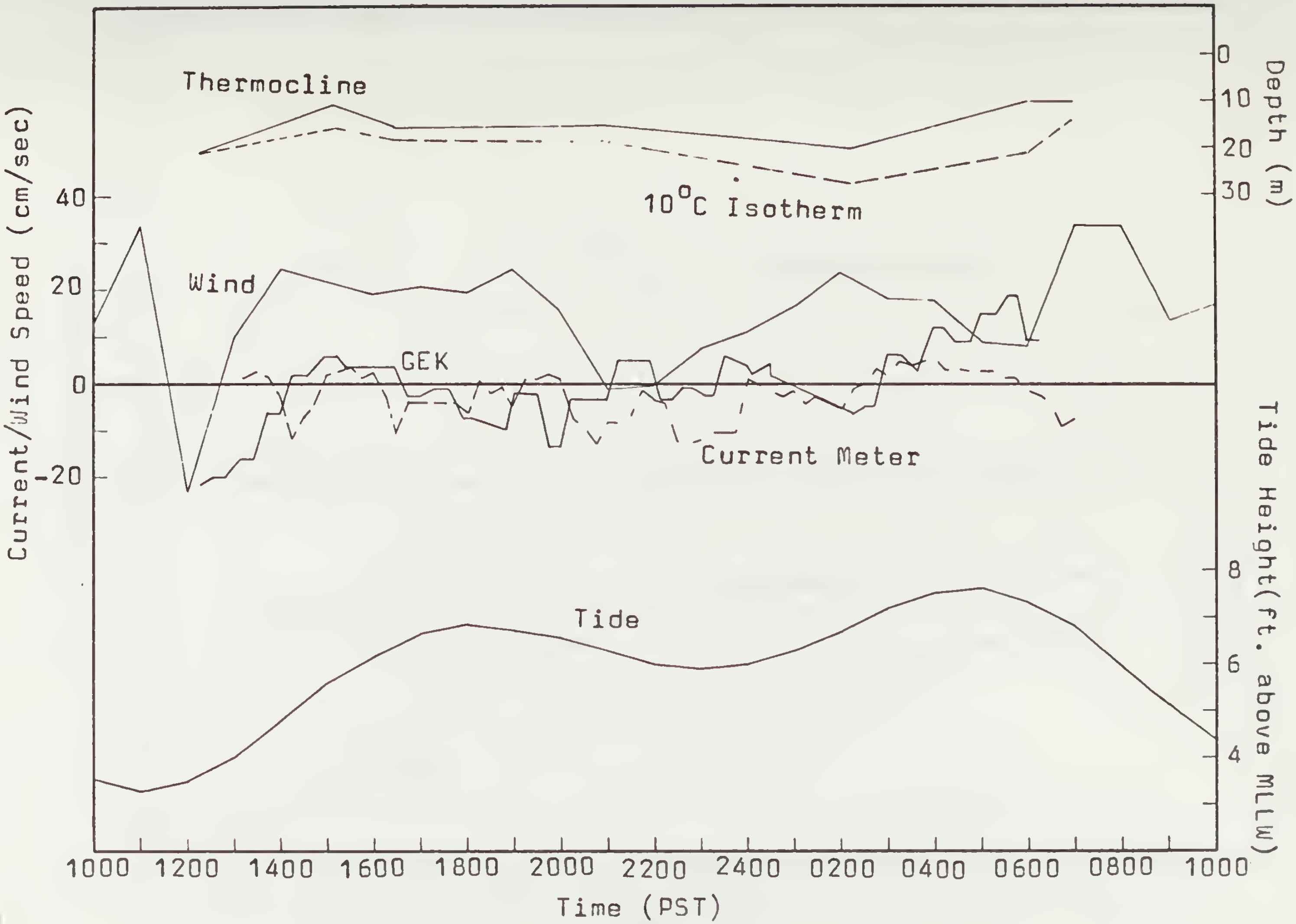

Figure 18. Run 3, North-Setting Components of GEK, Current Meter, and Wind, Tide Height, and Depth of Thermocline and 10°C Isotherm. For wind speed, read 10 times scale reading; for current meter speed, read 1/5 scale reading.

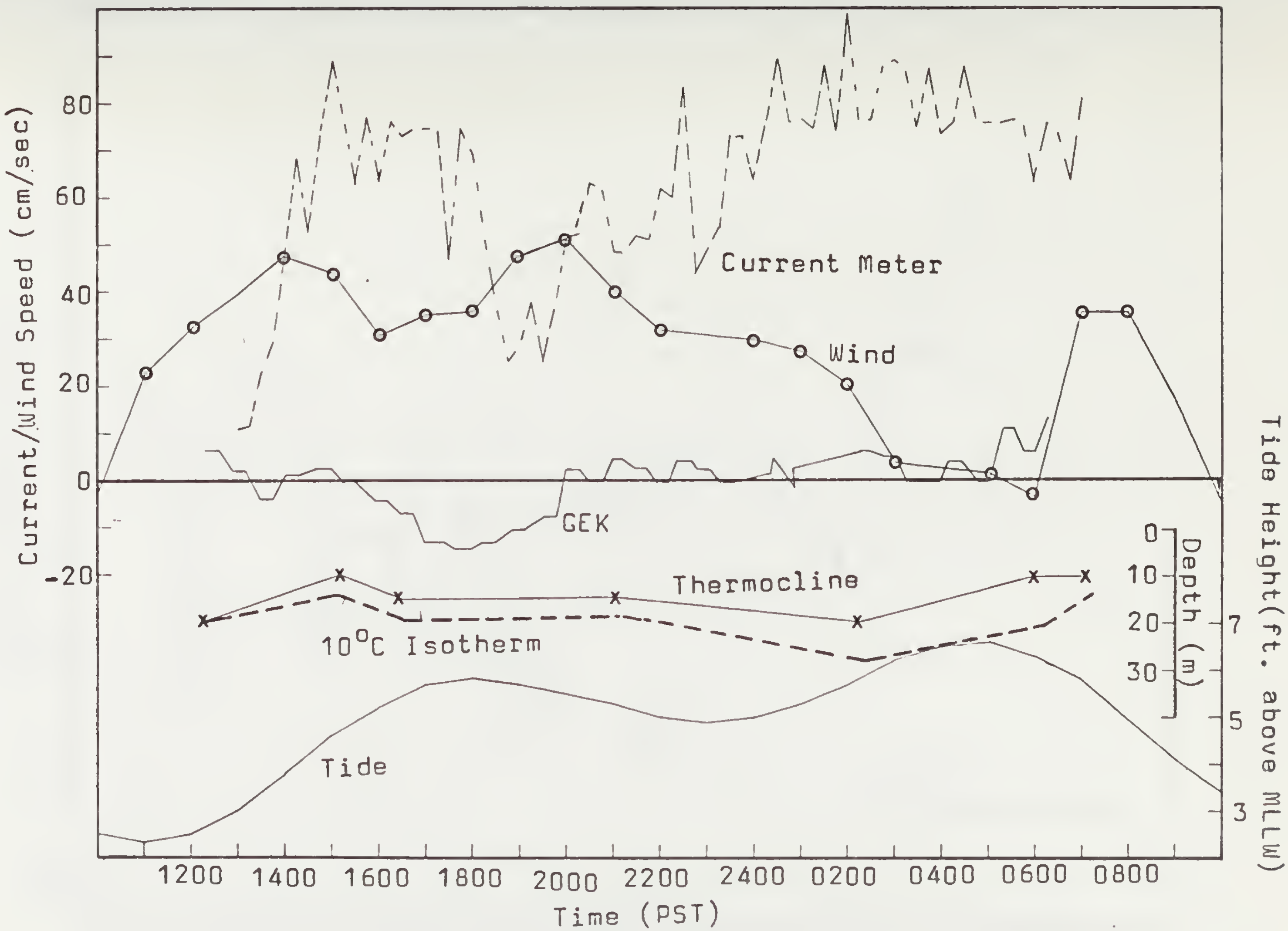

Figure 19. Run 3, East-Setting Components of GEK, Current Meter, and Wind, Tide Height, and Depth of Thermocline and 10°C Isotherm. For wind speed, read 10 times scale reading; for current meter speed, read 1/5 scale reading.

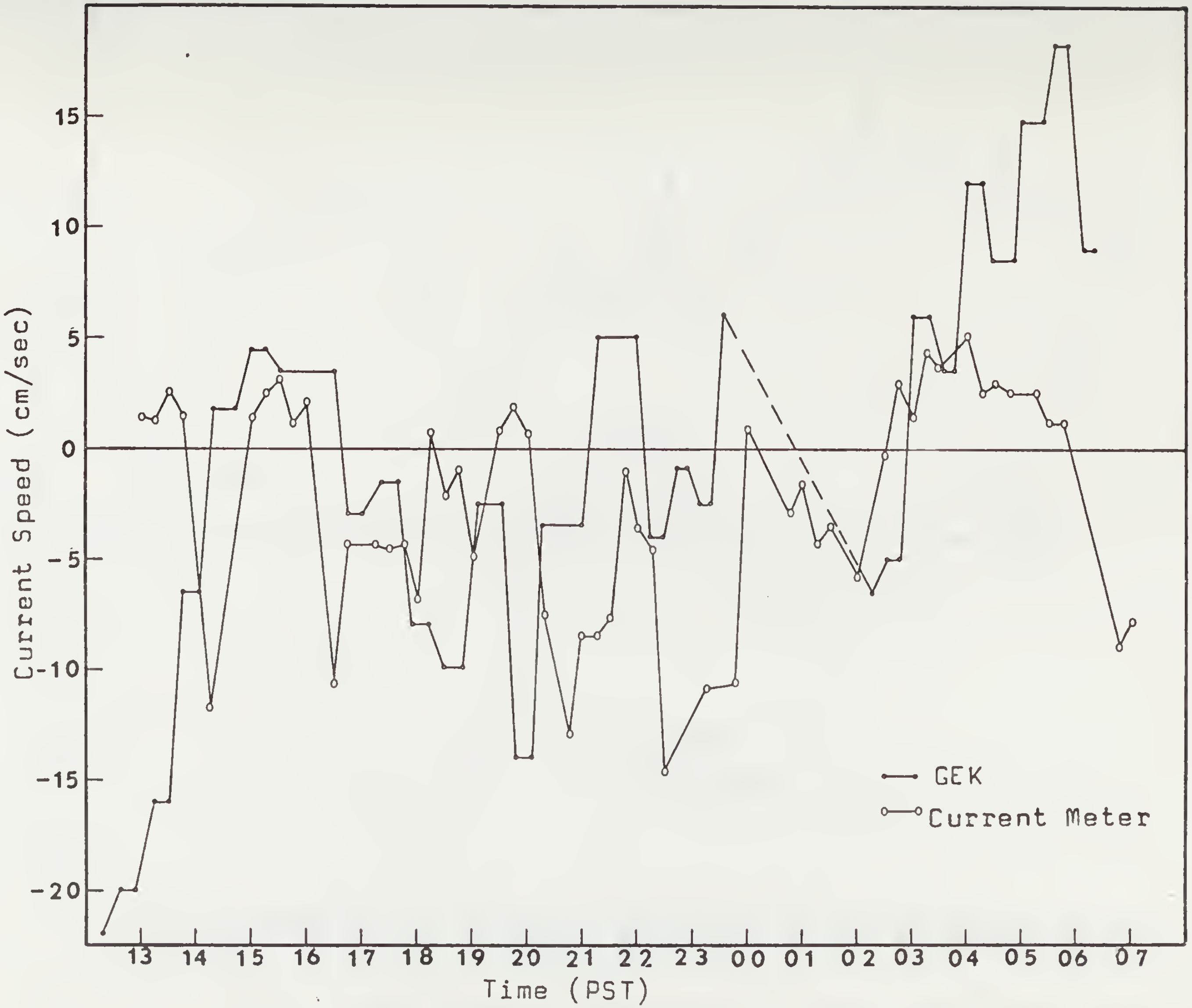

Figure 20. Run 3, North-Setting Components of GEK and Current Meter.

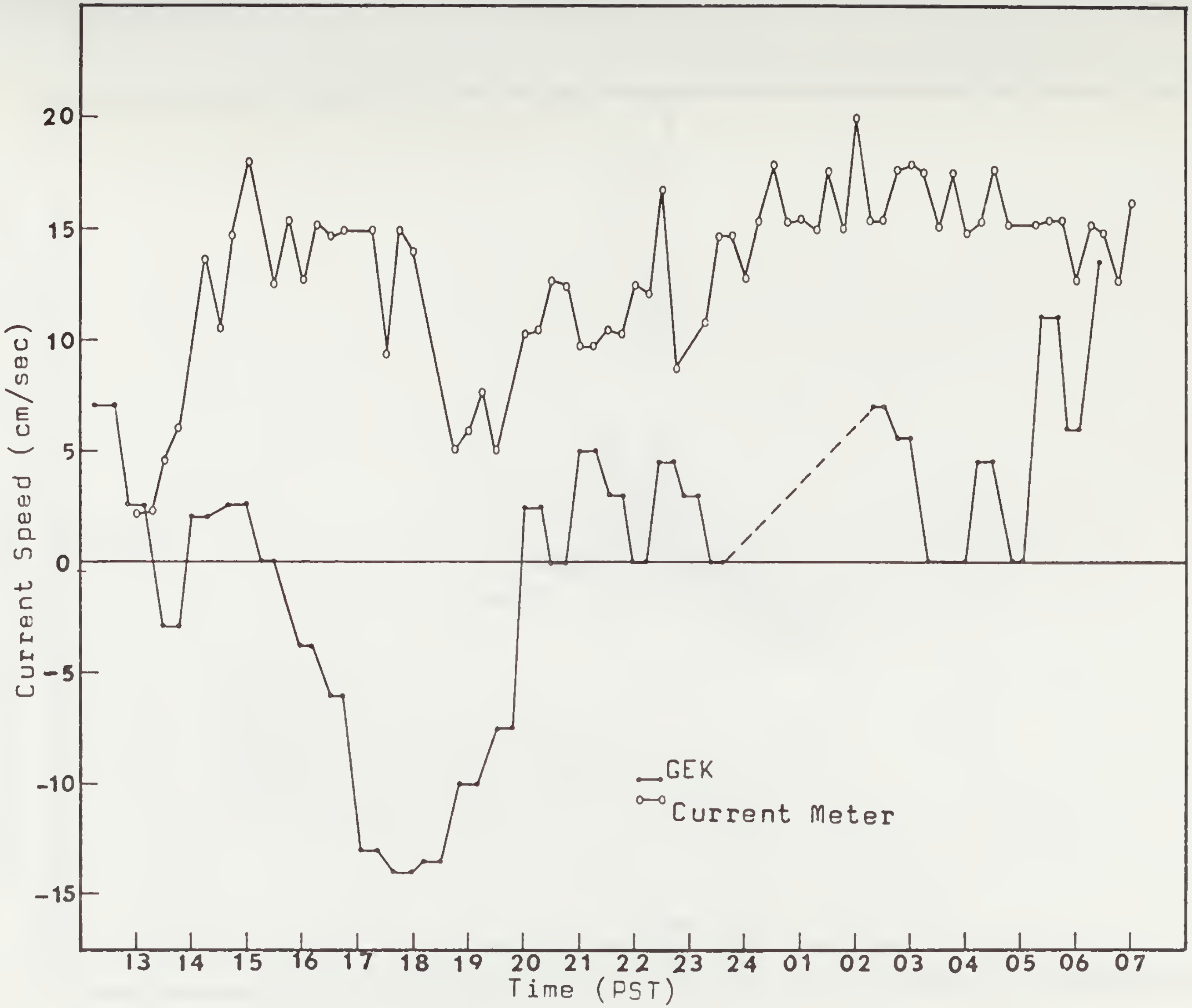

Figure 21. Run 3, East-Setting Components of GEK and Current Meter.

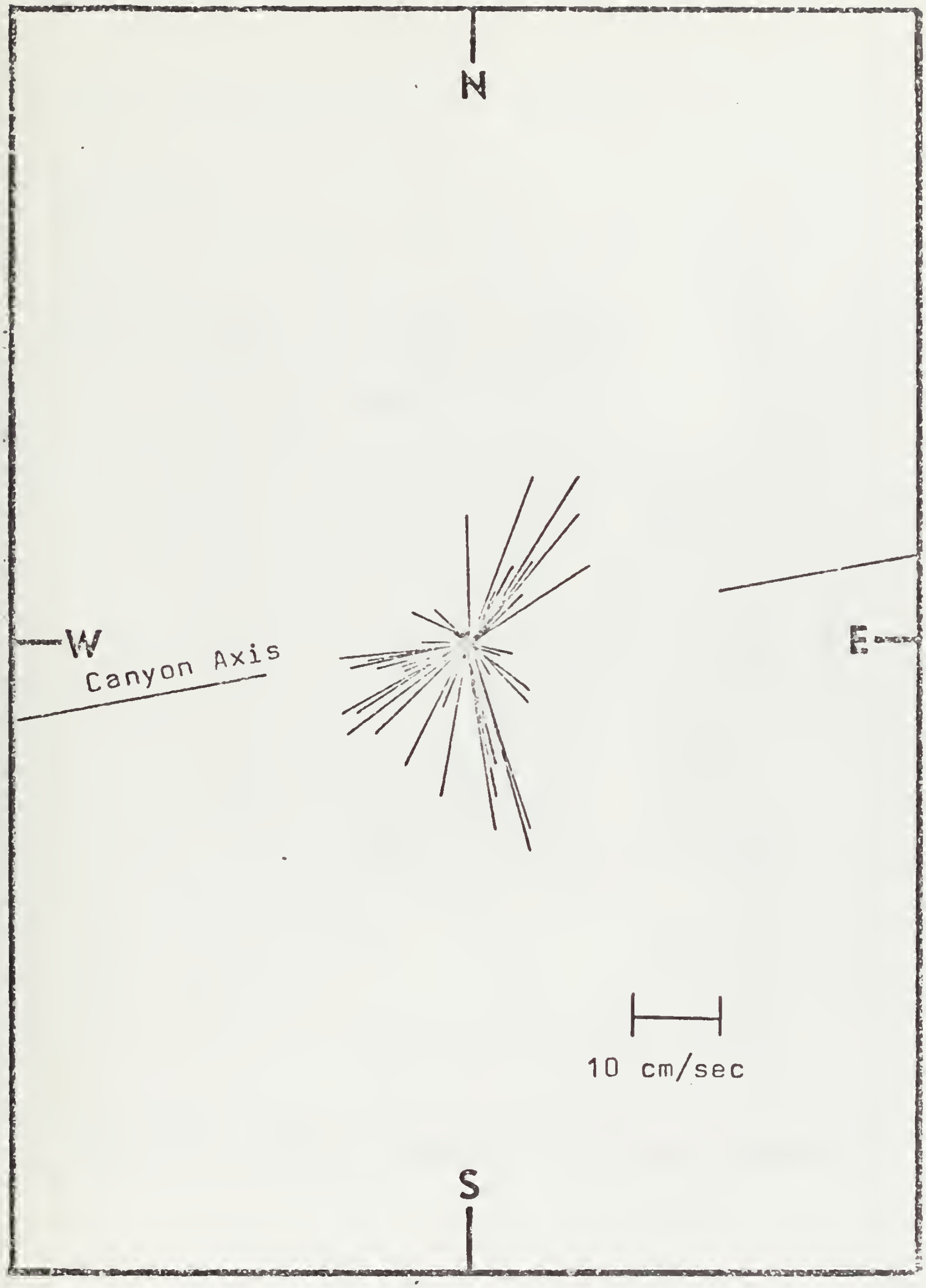

Figure 22. Run 3, Vector Scatter Diagram

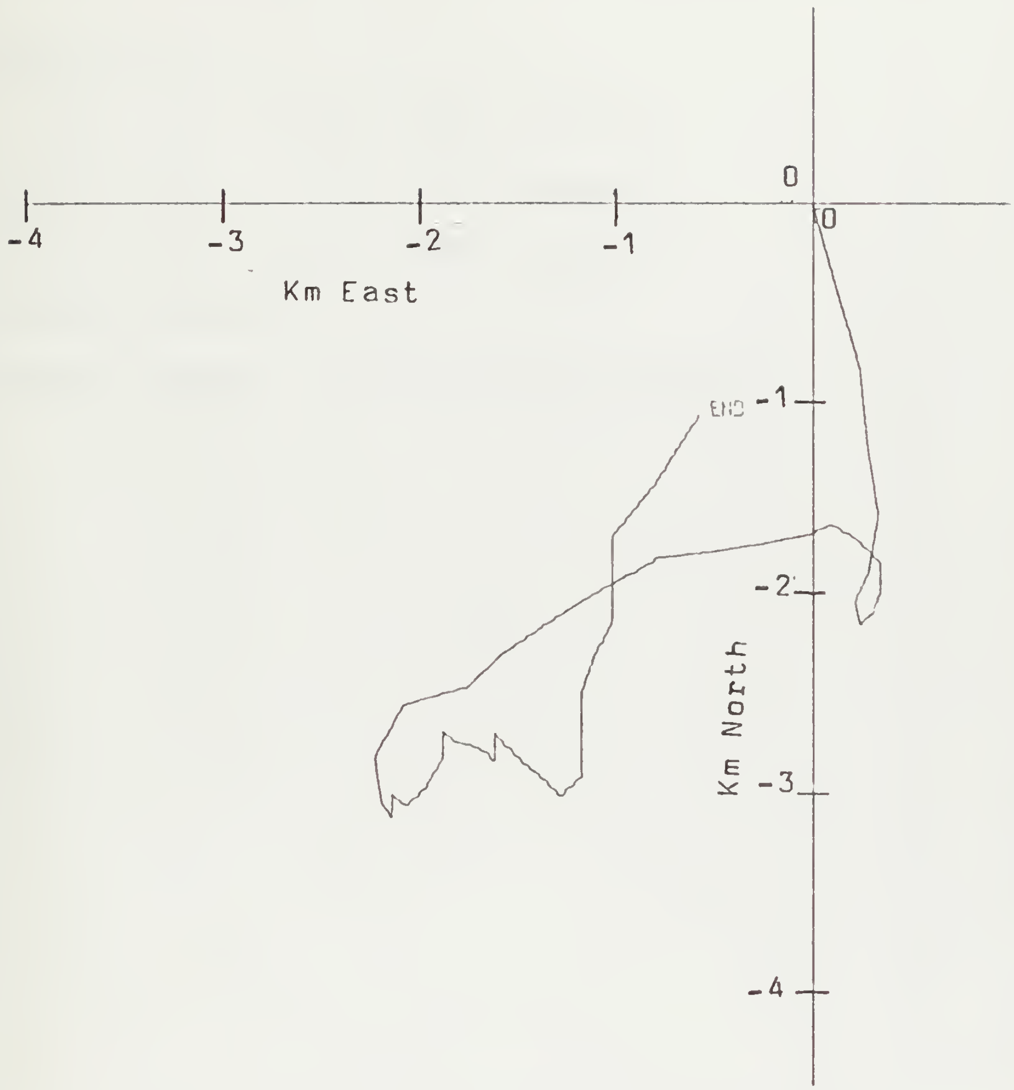

Figure 23. Run 3, Progressive Vector Diagram

D. RUN FOUR

Date: 0900, 21 April 1975 - 0900, 22 April 1975

Coordinates:

A- 36° - 47.1'N, 121° - 53.7'W

B- 36° - 47.1'N, 121° - 54.8'W

C- 36° - 47.8'N, 121° - 54.8'W

54 Data Points

Vector Average: 9.79 cm/sec @ 158.5°T

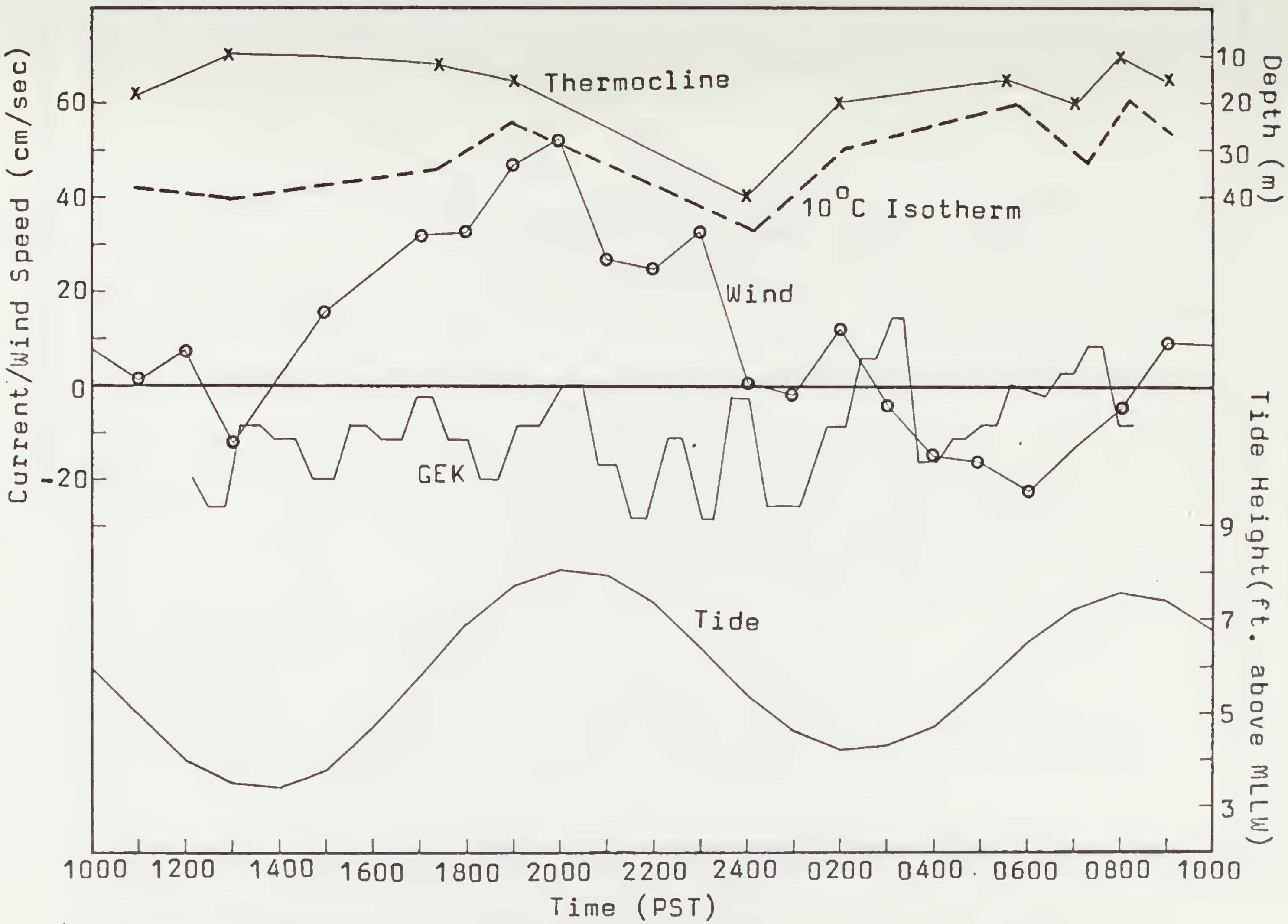

Figure 24. Run 4, North-Setting Components of GEK and Wind, Tide Height, and Depth of Thermocline and 10°C Isotherm. For wind speed, read 10 times scale reading.

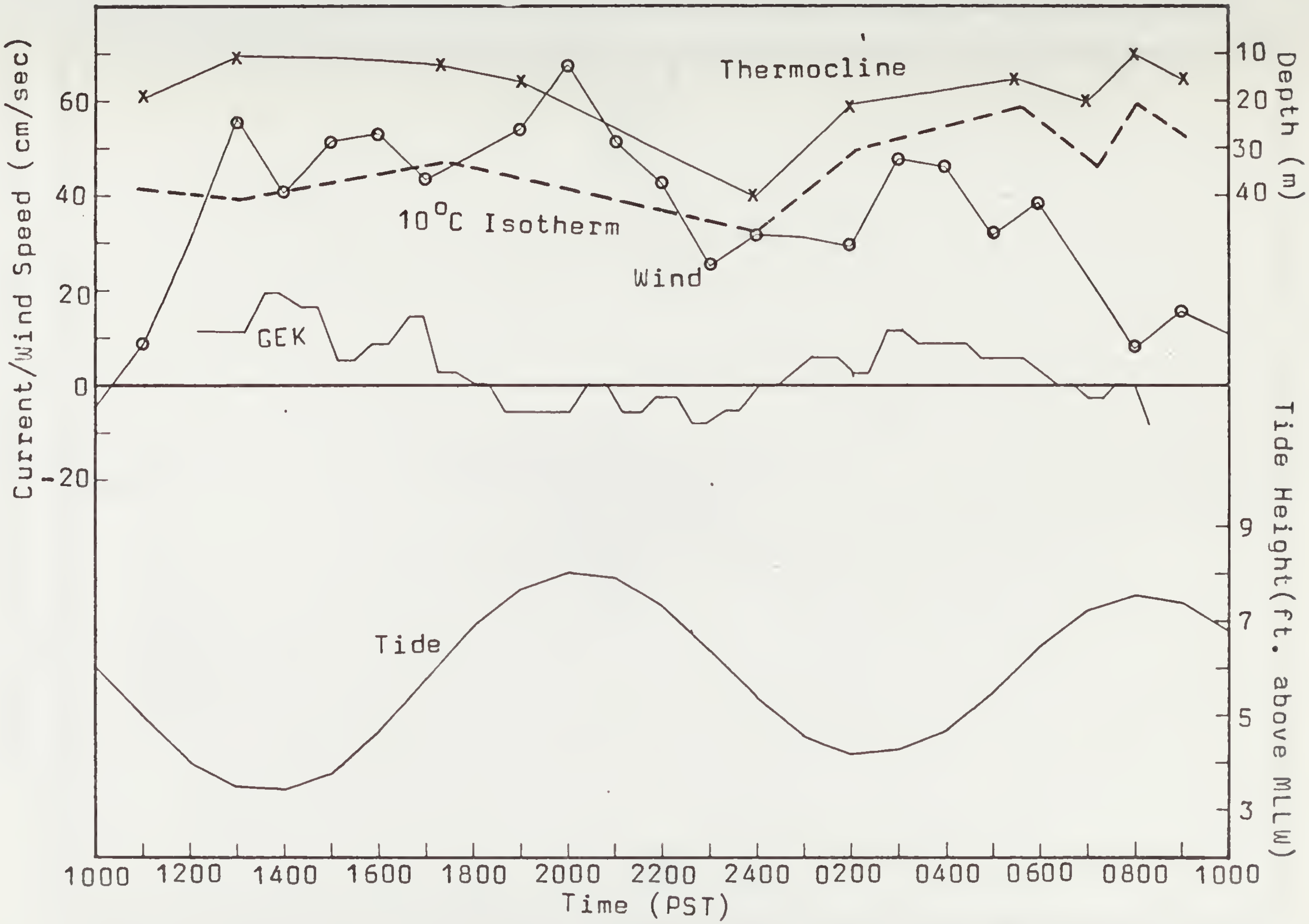

Figure 25. Run 4, East-Setting Components of GEK and Wind, Tide Height, and Depth of Thermocline and 10°C Isotherm. For wind speed, read 10 times scale reading.

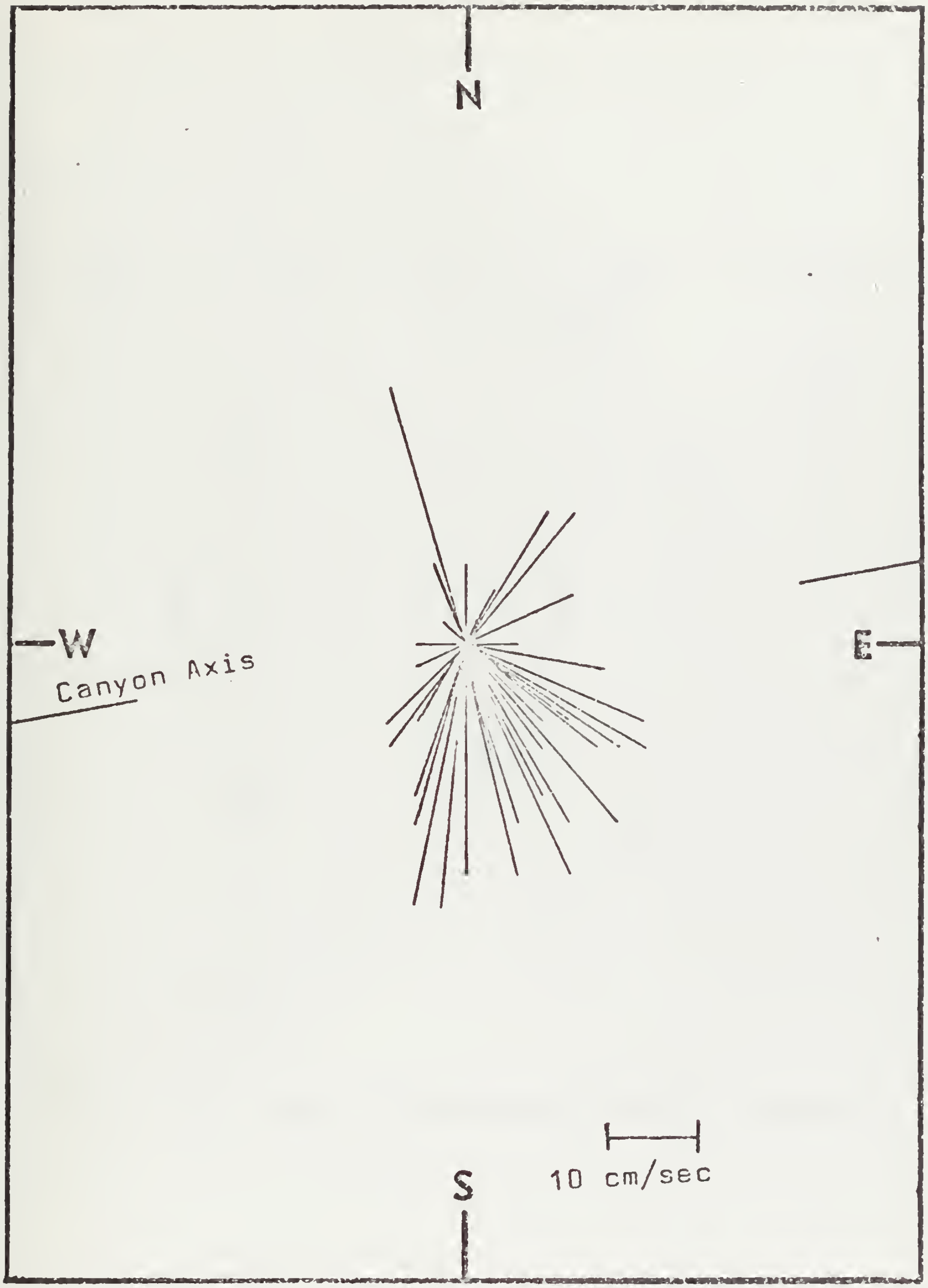

Figure 26. Run 4, Vector Scatter Diagram

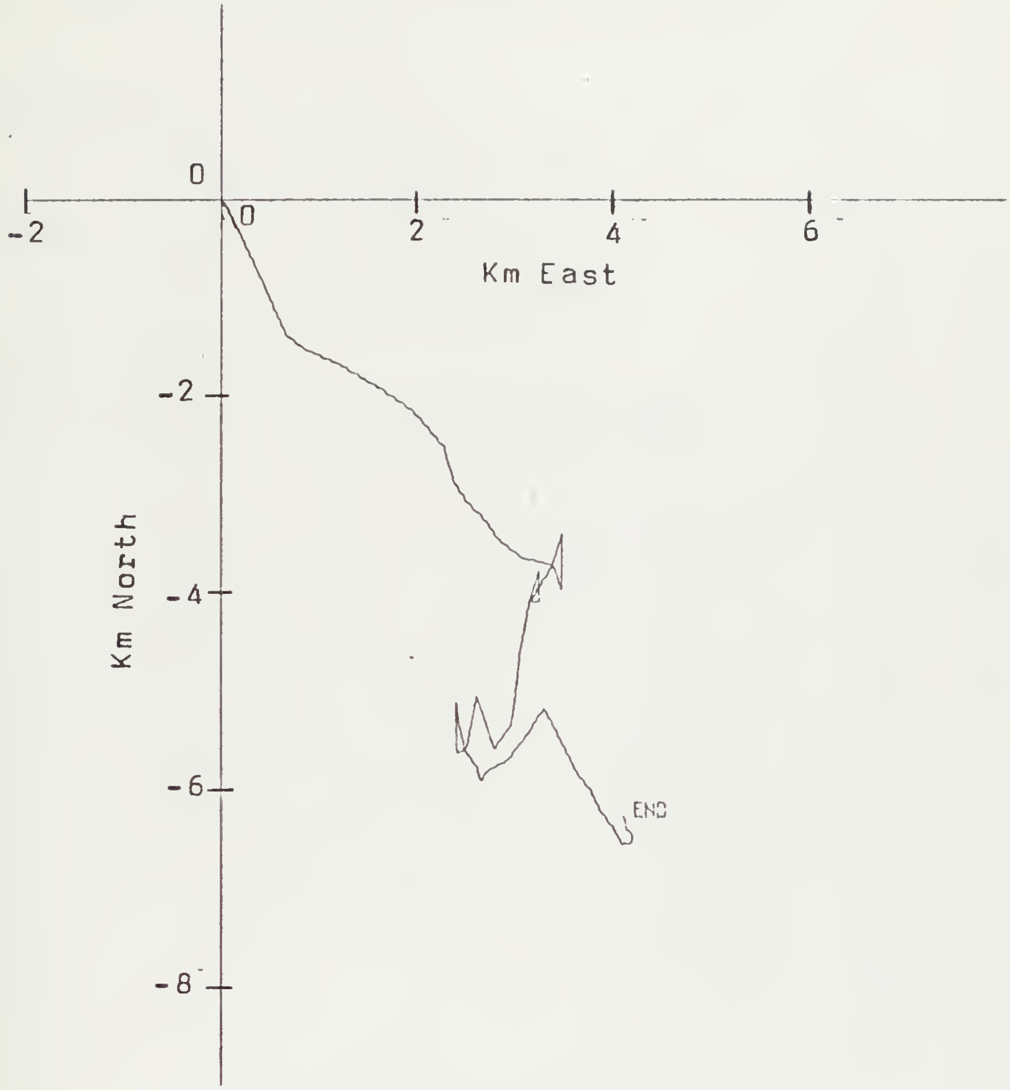

Figure 27. Run 4, Progressive Vector Diagram

E. RUN FIVE

Date: 0900, 1 May 1975 - 0900, 2 May 1975

Coordinates:

A- 36° - 47.1'N, 121° - 53.3'W

B- 36° - 47.1'N, 121° - 54.2'W

C- 36° - 47.9'N, 121° - 54.2'W

61 Data Points

Vector Average: 13.68 cm/sec @ 175.75°T

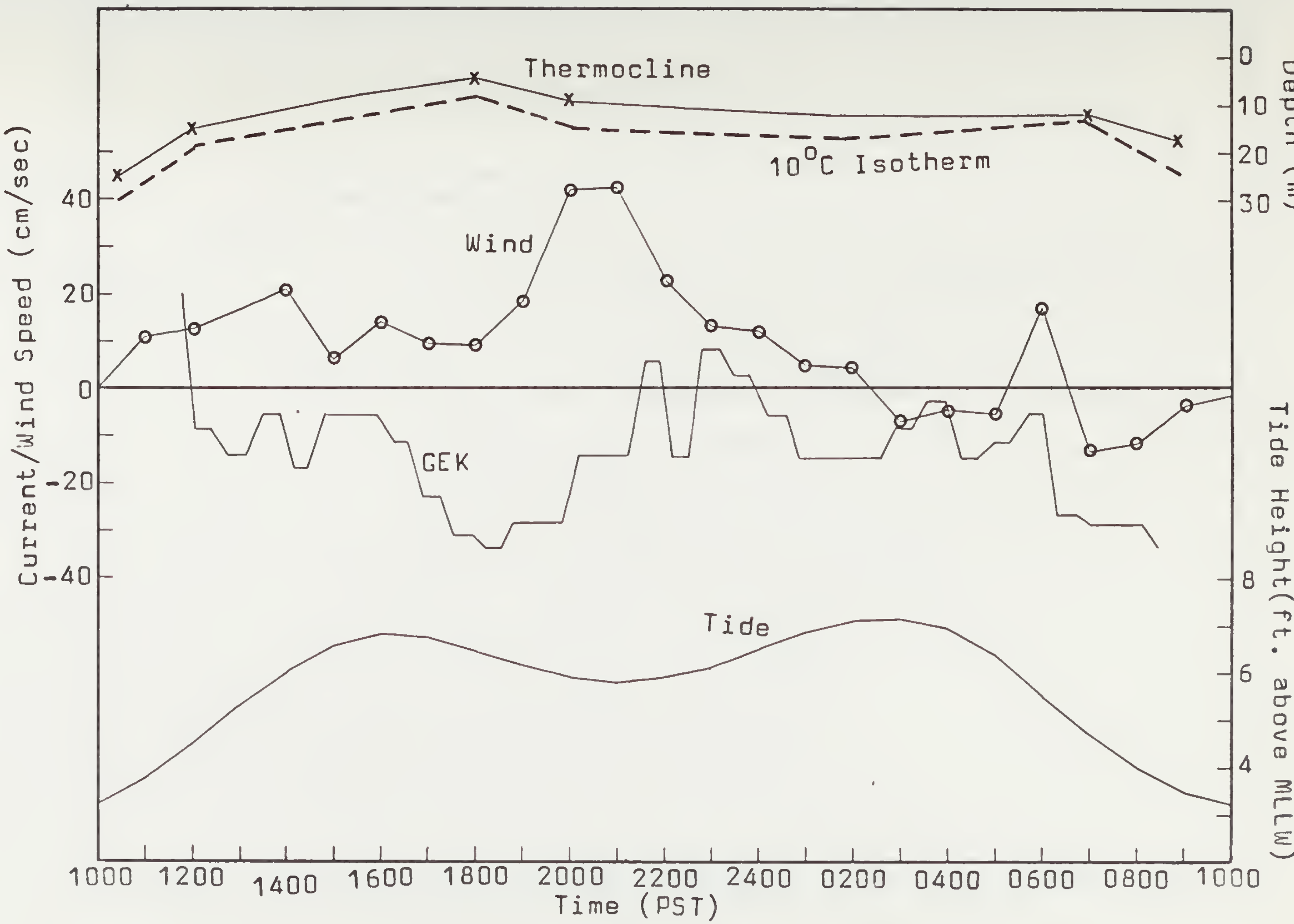

Figure 28. Run 5, North-Setting Components of GEK and Wind, Tide Height, and Depth of Thermocline and 10°C Isotherm. For wind speed, read 10 times scale reading.

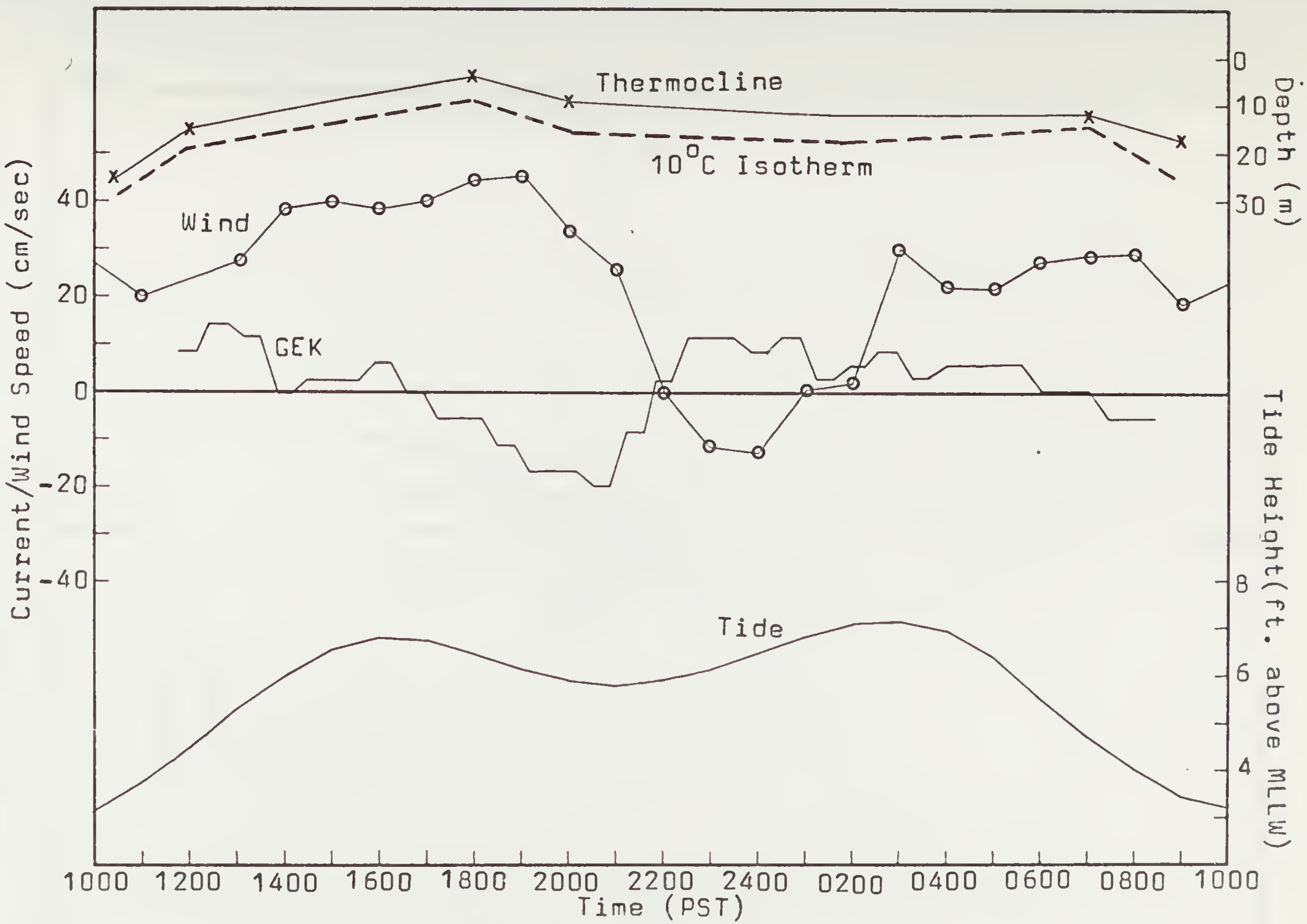

Figure 29. Run 5, East-Setting Components of GEK and Wind, Tide Height, and Depth of Thermocline and 10°C Isotherm. For wind speed, read 10 times scale reading.

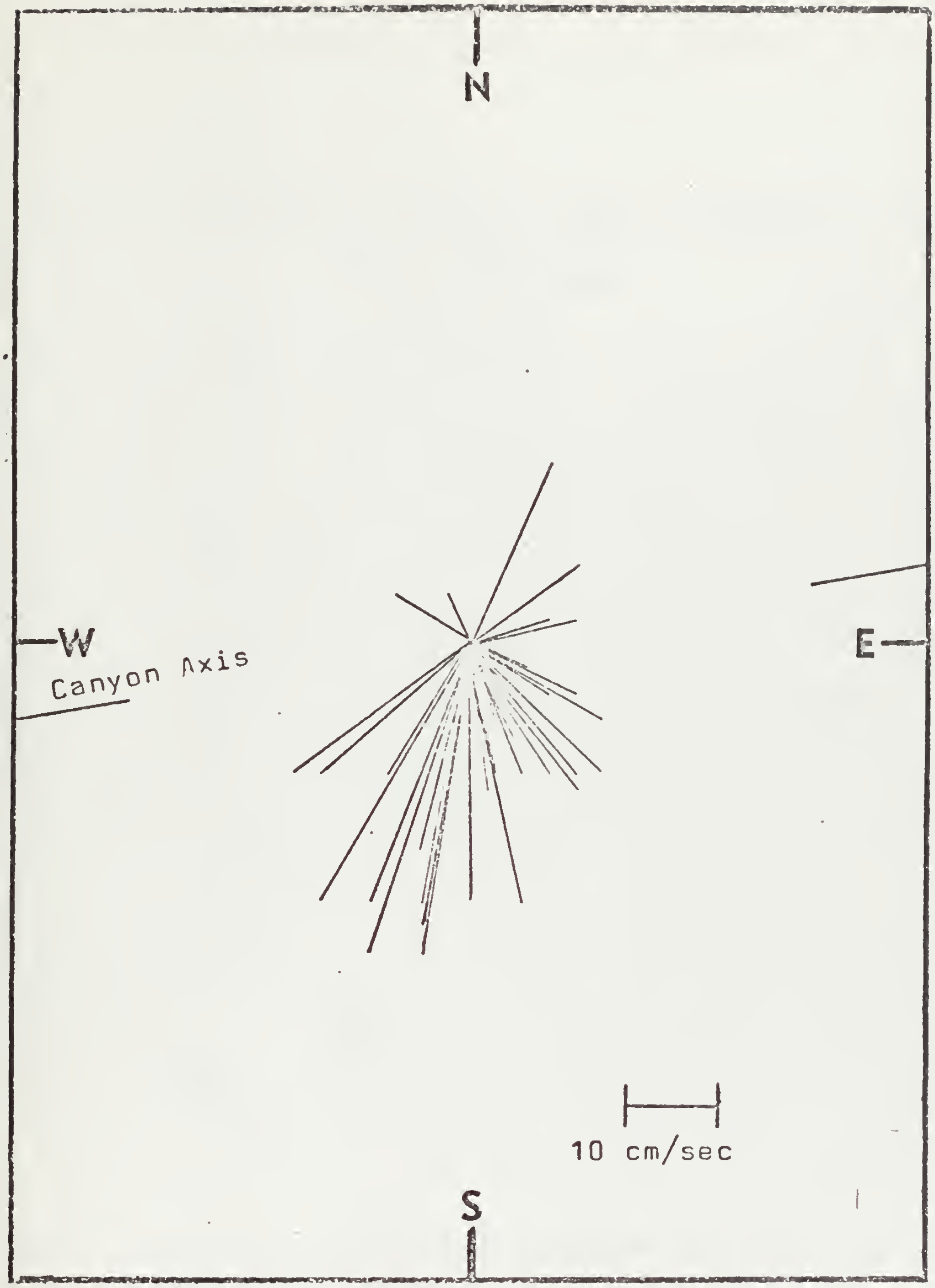

Figure 30. Run 5, Vector Scatter Diagram

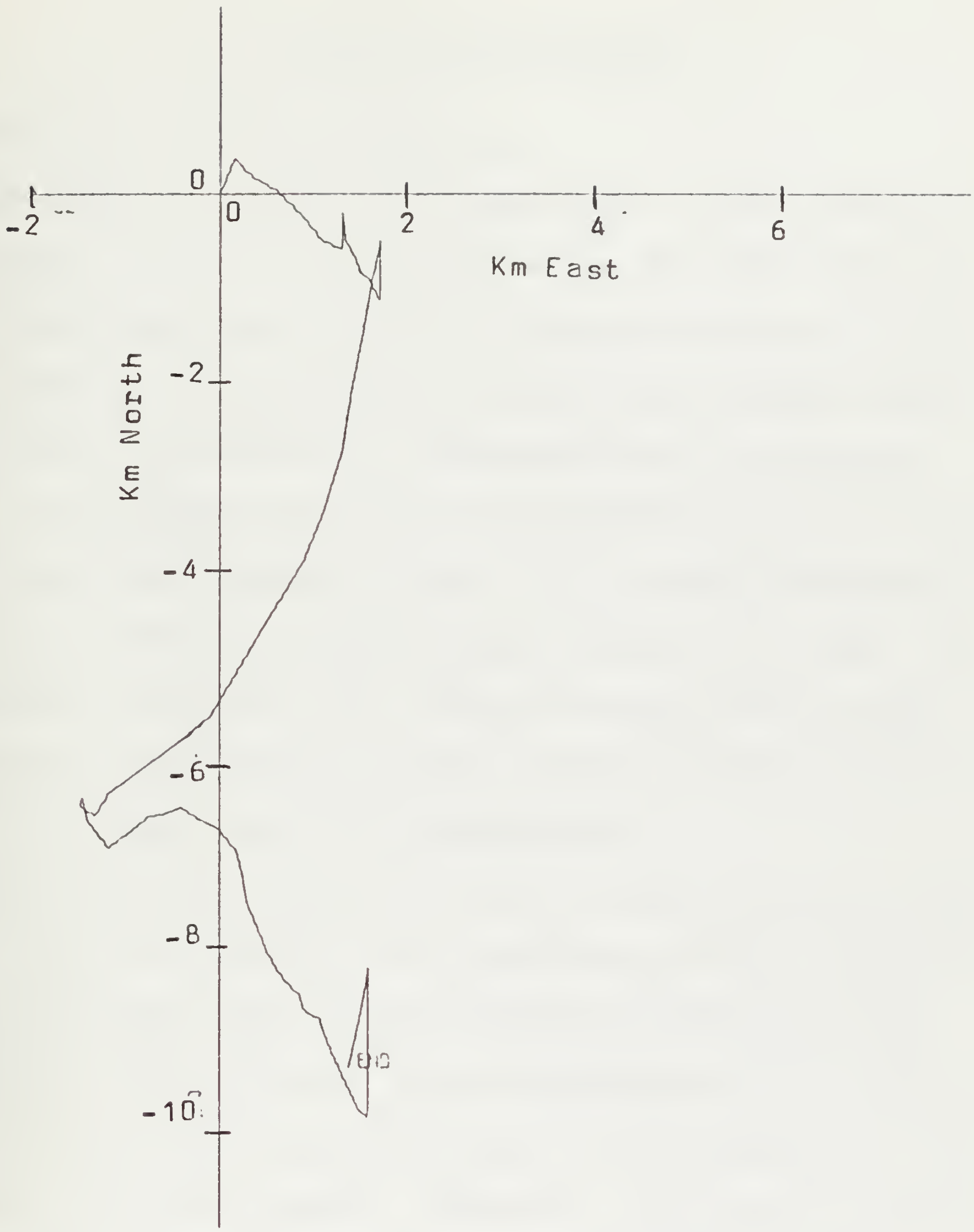

Figure 31. Run 5, Progressive Vector Diagram

V. DISCUSSION OF RESULTS

A. VALIDITY OF THE MEASUREMENTS

The apparent disparity in magnitudes of the surface and subsurface currents as recorded during Run Three provoked some doubt about the validity of the GEK records. The recorder was not in appreciable error; recalibration showed it to read 5 percent low. Two conclusions are possible. Either the currents measured in the thermocline are poorly correlated with surface currents, or the GEK measurements are poorly correlated with surface currents, or both. In principle, the flow in the thermocline need not be well-correlated with surface currents because of the low eddy viscosity at the top of the thermocline.

The mean flows obtained by three workers [McKay, 1970, Smith, 1972, and Howton, 1972] obtained with the GEK over the canyon range from 11 to 13 cm/sec and are generally southerly. These results agree satisfactorily with those of the present work shown in Table IV, considering the variations of day and season. Therefore, the present data are comparable with the GEK data of the past, and no error peculiar to the present series seems likely.

Scott [1973], quoting the data of AMBAG (Association of Monterey Bay Area Governments) personnel obtained with drogues, shows average currents of 7-10 cm/sec over and near the canyon in June. This agrees approximately with the present data and

suggests that no large k-factor is necessary to convert the data. Thus, although no precise k-factor can be assigned, it seems justifiable to speak of the GEK measurements as "currents" and to assume that k equals 1.0 pending a more precise determination.

TABLE IV

Averaged Data

Run	Speeds (cm/sec)			Avg Dir (°T)
	Avg N	Avg E	Avg Magn	
1	-8.33	4.33	9.39	152.5
2	-5.37	-5.19	7.47	226.0
3	-0.69	-0.02	.69	180.0
4	-9.10	3.61	9.79	155.5
5	-13.64	1.02	13.68	175.75

B. DISCUSSION OF DATA

The various composite graphs were examined visually for evidence of correlation between parameters. As was mentioned previously, such short data sets could not be analyzed statistically for periods approximating half the length of time-series with any validity unless the signal-to-noise ratio were large. This is equivalent to saying that the correlation would be obvious to visual examination. Although the parameters contain components of the order of a 12-hour period, it is clear that none of them is correlated.

The probable influence of magnetic storms on Run 1 was discussed in Section II. The effects of these storms appear

smaller than those predicted theoretically. The likelihood that the apparent currents represented real surface currents was discussed in Section V-A. It was concluded that they are less than real currents, on the average, by a factor between one and two. The average currents agree reasonably well with previous measurements in the area with the GEK.

APPENDIX A

PROGRAMS AND DATA TABLES

```
C                                PROGRAM KAMGEEK
C
C     CONVERTS CURRENTS IN N AND E COMPONENTS TO VECTOR FORM
C     AND TIME TO DECIMAL FORM CONTINUOUS OVER THE
C     0000-2400 BOUNDARY
C
      DIMENSION TIME1(4),TIME2(4),V(4),U(4),TIME(4),XMAG(4),
     *DIR(4)
      K=4
      PI=3.14592
      RAD=180./PI
      TP=0.
      ADD=0.
      XK=60.
      N=0
      WRITE(6,200)
      WRITE(6,300)
C
    1 READ(5,5)(TIME1(J),TIME2(J),V(J),U(J), J=1,4)
    5 FORMAT(4(2F2.0,2F7.1))
      DO 15 J=1,K
      IF(TIME1(J).EQ.99)GO TO  6
      IF(TIME2(J).EQ.0.)TIME2(J)=1.E-5
    2 TIME(J)=TIME1(J)+TIME2(J)/XK
      IF((TP-TIME(J)).GT.20.) ADD=24.
      TIME(J)=TIME(J)+ADD
      IF(TIME(J).GT.24.) TIME(J)=TIME(J)-24.
      TP=TIME1(J)
      XMAG(J)=SQRT(U(J)*U(J)+V(J)*V(J))
      IF(XMAG(J).EQ.0.)XMAG(J)=1.E-5
      DIR(J)=ABS(ARSIN(U(J)/XMAG(J)))
      IF(U(J).GT.0..AND.V(J).GT.0.)DIR(J)=DIR(J)
      IF(U(J).LT.0..AND.V(J).GT.0.)DIR(J)=2.*PI-DIR(J)
      IF(U(J).LT.0..AND.V(J).LT.0.)DIR(J)=1.*PI+DIR(J)
      IF(U(J).GT.0..AND.V(J).LT.0.)DIR(J)=1.*PI-DIR(J)
      JJ=J
      DIR(J)=DIR(J)*RAD
   15 CONTINUE
      GO TO 25
    6 JJ=JJ-1
  100 FORMAT(24X,F5.2,8X,F5.1,8X,F4.0)
  200 FORMAT(24X,'TIME',7X,'MAGNITUDE',4X,'DIRECTION')
  300 FORMAT(23X,'(LOCAL)',6X,'(CM/SEC)',3X,'(DEG TRUE)',/)
      WRITE(6,100)(TIME(J),XMAG(J),DIR(J),J=1,JJ)
      WRITE(7,100)(TIME(J),XMAG(J),DIR(J),J=1,JJ)
      GO TO 45
   25 WRITE(6,100) (TIME(J),XMAG(J),DIR(J),J=1,4)
      WRITE(7,100) (TIME(J),XMAG(J),DIR(J),J=1,4)
   30 GO TO 1
   45 CONTINUE
      STOP
      END
```

Figure A-1. Program KAM GEEK

TABLE A-I

Run 1, GEK Data

TIME (LOCAL)	MAGNITUDE (CM/SEC)	DIRECTION (DEG TRUE)
15.75	52.1	189.
16.03	41.4	191.
16.37	40.6	0.
16.67	22.3	0.
16.98	30.6	137.
17.28	41.6	150.
17.63	40.3	153.
17.92	36.2	150.
18.20	40.0	141.
18.48	32.3	129.
18.77	32.8	128.
19.05	34.5	132.
19.33	34.0	133.
19.65	30.3	124.
19.95	40.9	115.
20.23	45.6	125.
20.52	43.0	128.
20.83	36.5	112.
21.13	30.9	116.
21.43	27.8	88.
21.73	14.9	87.
22.02	15.6	72.
22.33	20.8	77.
22.67	20.3	86.
22.98	20.3	86.
23.30	25.2	126.
23.62	15.6	163.
23.95	4.7	90.
0.23	8.1	90.
0.53	10.6	230.
0.82	22.7	253.
1.08	23.4	292.
1.35	9.0	13.
1.67	29.2	4.
2.02	29.4	8.
2.30	7.3	146.
2.60	7.0	209.
2.92	8.1	205.
3.22	7.7	195.
3.52	9.0	193.
3.83	19.1	242.
4.15	20.4	236.
4.45	11.8	193.
4.83	36.0	356.
5.18	38.4	339.
5.47	35.8	338.
5.72	34.7	343.
6.02	18.6	213.
6.30	16.0	192.
6.58	37.4	185.
7.23	53.2	187.
7.52	7.3	292.
7.80	17.8	279.
8.12	78.5	347.
8.47	77.5	351.
8.78	12.4	261.
9.10	7.1	254.
9.40	41.2	189.
9.73	40.6	0.
10.00	45.4	0.
10.30	45.7	187.
10.62	13.3	336.
10.88	12.9	341.
11.15	13.5	342.
11.47	13.3	15.

TABLE A-II

Run 1, Wind Data

TIME PDT	DIRECTION °T	SPEEDS (CM/SEC) SCALAR	EAST COMPONENT	NORTH COMPONENT
1000	130	89.4	-68.48	57.48
1100	120	89.4	-77.42	44.7
1200	073	223.5	-65.26	-213.67
1300	293	357.6	328.99	139.82
1400	314	312.9	224.98	-217.47
1500	308	268.2	211.34	-165.21
1600	316	312.9	224.98	-217.47
1700	230	268.2	172.45	205.44
1800	062	447.0	-209.64	-394.70
1900	069	491.7	-176.03	-459.25
2000	074	491.7	-135.71	-472.52
2100	072	357.6	-110.50	-340.08
2200	060	670.5	-335.25	-580.65
2300	066	536.4	-218.31	-490.27
2400	076	402.3	-97.36	-390.23
0100	081	357.6	-55.79	-353.31
0200	094	402.3	-401.50	28.16
0300	083	491.7	-59.99	-488.26
0400	089	402.3	-6.84	-401.90
0500	078	357.6	-74.38	-349.73
0600	088	268.2	-9.39	-267.93
0700	096	268.2	-266.86	28.16
0800	098	223.5	-221.27	31.07
0900	108	268.2	-255.06	82.87
1000	103	134.1	-130.61	30.17
1100	088	223.5	-7.82	-223.28
1200	125	134.1	-109.83	76.97

TABLE A-III

Run 2, GEK Data

TIME (LOCAL)	MAGNITUDE (CM/SEC)	DIRECTION (DEG TRUE)
10.45	2.0	33.
10.92	17.0	276.
11.38	16.9	90.
11.78	20.3	90.
12.22	24.4	304.
12.65	16.0	328.
13.08	32.1	345.
13.55	33.0	340.
13.97	22.8	330.
14.42	20.0	8.
14.85	8.9	18.
15.37	14.1	53.
16.07	12.6	64.
16.78	10.2	57.
17.22	32.1	165.
17.73	32.1	165.
18.23	45.9	169.
19.03	45.4	173.
19.42	42.7	172.
19.88	43.1	191.
20.33	26.8	162.
20.78	27.8	204.
21.30	22.8	210.
21.77	28.0	225.
22.25	24.3	234.
22.72	24.3	234.
23.18	20.6	286.
23.65	26.0	283.
0.13	30.5	304.
0.58	30.5	304.
1.07	29.1	299.
1.55	24.3	306.
2.02	24.3	306.
2.53	19.9	315.
3.02	16.4	239.
3.52	18.9	243.
3.98	17.8	252.
4.43	10.2	237.
4.88	12.0	225.
5.35	10.2	213.
5.75	7.9	225.
6.17	10.2	123.
6.57	14.1	143.
7.03	27.8	114.
7.50	32.2	128.
7.87	26.0	140.
8.43	22.0	130.
8.98	15.2	158.
9.37	12.6	154.

TABLE A-IV

Run 2, Wind Data

TIME PDT	DIRECTION °T	SPEEDS (CM/SEC) SCALAR	EAST COMPONENT	NORTH COMPONENT
1000	110	178.8	-167.54	61.15
1100	168	89.4	-18.60	87.43
1200	130	134.1	-86.23	102.72
1300	277	312.9	310.71	-38.13
1400	294	402.3	367.70	-163.74
1500	273	357.6	357.11	-18.60
1600	255	357.6	345.44	92.62
1700	170	223.5	-38.89	220.15
1800	187	312.9	38.17	310.71
1900	178	134.1	-4.69	133.97
2000	118	178.8	-157.88	83.86
2100	156	89.4	-36.39	81.71
3300	184	44.7	3.13	44.61
2300	110	134.1	-126.05	45.86
2400	177	178.8	-9.30	178.44
0100	331	402.3	195.12	-352.01
0200	221	223.5	146.62	168.74
0300	131	89.4	-67.50	58.65
0400	100	178.8	-168.07	61.15
0500	095	223.5	-222.61	19.44
0600	139	44.7	-29.32	33.75
0700	093	268.2	-267.93	13.95
0800	095	312.9	-311.65	27.22
0900	081	223.5	-220.82	-34.87
1000	206	44.7	19.58	40.19
1100	252	44.7	42.51	13.81
1200	274	89.4	89.22	-6.26

TABLE A-V

Run 3, GEK Data

TIME (LOCAL)	MAGNITUDE (CM/SEC)	DIRECTION (DEG TRUE)
12.30	22.9	164.
12.62	21.8	163.
12.90	21.0	174.
13.18	17.1	172.
13.47	17.2	191.
13.77	7.6	207.
14.07	7.0	166.
14.33	2.4	45.
14.65	2.9	53.
14.97	6.1	22.
15.27	5.6	0.
15.58	3.4	0.
15.87	5.2	311.
16.17	5.2	311.
16.47	7.1	299.
16.73	6.8	246.
17.02	13.3	258.
17.35	13.1	262.
17.65	14.2	263.
17.95	16.2	241.
18.22	15.6	240.
18.53	16.6	235.
18.82	14.0	227.
19.10	10.5	257.
19.47	7.7	252.
19.77	15.3	208.
20.02	13.7	170.
20.25	4.1	146.
20.52	3.4	0.
20.75	3.4	0.
20.98	5.6	127.
21.23	6.4	45.
21.47	5.3	32.
21.68	5.3	32.
21.95	4.5	0.
22.17	3.4	0.
22.42	5.6	127.
22.67	4.6	104.
22.88	3.0	112.
23.10	4.0	135.
23.33	2.8	0.
23.53	5.6	0.
2.25	9.6	135.
2.48	8.8	130.
2.75	7.9	135.
3.03	7.9	45.
3.32	5.6	0.
3.55	3.4	0.
3.75	3.4	0.
3.97	11.9	0.
4.20	12.7	21.
4.45	9.6	28.
4.83	8.5	0.
5.05	14.1	0.
5.35	18.1	39.
5.57	21.3	32.
5.80	19.3	21.
6.05	11.3	37.

TABLE A-VI

Current Meter Data

TIME (PST)	CURRENT METER READING MAGN (cm/sec)/DIR (°T)	COMPONENT SPEED E(cm/sec)	COMPONENT SPEED N(cm/sec)
1300	2.6 / 056	2.2	1.4
1315	2.6 / 061	2.2	1.3
1330	5.2 / 061	4.5	2.5
1345	6.2 / 076	6.0	1.5
1400	10.2 / 106	9.8	-2.9
1415	18.0 / 131	13.6	-11.8
1430	12.9 / 126	10.5	-7.6
1445	15.5 / 106	14.8	-4.3
1500	18.0 / 086	17.8	1.3
1515	15.5 / 081	15.2	2.5
1530	12.9 / 076	12.5	3.1
1545	15.5 / 086	15.3	1.1
1600	12.9 / 081	12.6	2.1
1615	15.5 / 101	15.2	-2.9
1630	18.0 / 126	14.6	-10.6
1645	15.5 / 106	14.9	-4.3
1700	15.5 / 106	14.9	-4.3
1715	15.5 / 106	14.9	-4.3
1730	10.3 / 116	9.3	-4.5
1745	15.5 / 106	14.9	-4.3
1800	15.5 / 116	13.9	-6.8
1815	10.3 / 086	10.2	0.7
1830	7.7 / 106	7.4	-2.2
1845	5.1 / 101	5.0	-1.0
1900	7.7 / 131	5.8	-5.0
1915	7.7 / 086	7.6	0.5
1930	5.1 / 081	5.0	0.8
1945	7.7 / 076	7.5	1.8
2000	10.3 / 086	10.2	0.7
2015	12.9 / 126	10.4	-7.6

TABLE A-VI (continued)

2030	15.5 / 126	12.6	-9.1
2045	18.0 / 136	12.4	-13.0
2100	12.9 / 131	9.7	-8.5
2115	12.9 / 131	9.7	-8.5
2130	12.9 / 126	10.4	-7.6
2145	10.3 / 096	10.2	-1.0
2200	12.9 / 106	12.4	-3.6
2215	12.9 / 111	12.0	-4.6
2230	20.6 / 126	16.7	-12.2
2245	15.5 / 146	8.7	-12.9
2300	15.5 / 141	9.8	-12.1
2315	15.5 / 136	10.7	-10.8
2330	18.0 / 126	14.6	-10.6
2345	18.0 / 126	14.6	-10.6
2400	12.9 / 086	12.7	0.9
0015	15.5 / 091	15.3	-0.3
0030	18.0 / 096	17.8	-1.8
0045	15.5 / 101	15.2	-2.9
0100	15.5 / 096	15.3	-1.6
0115	15.5 / 106	14.9	-4.3
0130	18.0 / 101	17.6	-3.4
0145	15.5 / 106	14.9	-4.3
0200	20.6 / 106	19.8	-5.8
0215	15.5 / 096	15.3	-1.6
0230	15.5 / 091	15.3	-0.3
0245	18.0 / 081	17.6	2.9
0300	18.0 / 086	17.8	1.3
0315	18.0 / 076	17.5	4.3
0330	15.5 / 076	15.0	3.6
0345	18.0 / 076	17.5	4.3
0400	15.5 / 071	14.7	5.1
0415	15.5 / 081	15.2	2.5
0430	18.0 / 081	17.6	2.9
0445	15.5 / 081	15.2	2.5

TABLE A-VI (continued)

0500	15.5 / 081	15.2	2.5
0515	15.5 / 081	15.2	2.5
0530	15.5 / 086	15.3	1.1
0545	15.5 / 086	15.3	1.1
0600	12.9 / 096	12.7	-1.3
0615	15.9 / 101	15.2	-2.9
0630	15.5 / 106	14.9	-4.3
0645	15.5 / 126	12.6	-9.1
0700	18.0 / 116	16.2	-7.9

TABLE A-VII

Run 3, Wind Data

TIME PDT	DIRECTION °T	SPEEDS (CM/SEC) SCALAR	EAST COMPONENT	NORTH COMPONENT
1000	166	134.1	-32.45	130.08
1100	213	402.3	219.25	337.53
1200	307	402.3	321.44	-242.18
1300	256	402.3	390.23	97.36
1400	243	536.4	477.93	243.53
1500	244	491.7	442.04	215.36
1600	238	357.6	303.24	189.53
1700	240	402.3	348.38	201.15
1800	241	402.3	352.01	195.12
1900	243	536.4	477.93	243.53
2000	253	536.4	512.80	156.63
2100	273	402.3	401.50	-20.92
2200	272	312.9	312.59	-10.95
2300	257	312.9	304.76	70.40
2400	251	312.9	295.69	102.00
0100	240	312.9	270.97	156.45
0200	222	312.9	209.33	232.48
0300	192	178.8	37.19	174.87
0400	188	178.8	24.85	177.01
0500	192	89.4	18.60	87.43
0600	154	89.4	-39.16	80.37
0700	227	491.7	359.43	335.34
0800	227	491.7	359.43	335.34
0900	232	223.5	176.12	137.68
1000	162	178.8	-55.25	170.04
1100	181	268.2	4.57	267.93
1200	220	357.6	229.94	273.92

TABLE A-VIII

Run 4, GEK Data

TIME (LOCAL)	MAGNITUDE (CM/SEC)	DIRECTION (DEG TRUE)
12.13	22.8	150.
12.45	27.8	156.
12.78	27.8	156.
13.15	14.1	127.
13.57	21.5	113.
13.88	22.8	120.
14.35	20.3	124.
14.72	26.0	140.
15.15	20.6	164.
15.50	10.2	147.
15.83	12.0	135.
16.18	14.1	143.
16.65	18.1	129.
16.97	14.4	101.
17.25	4.0	135.
17.63	11.6	166.
18.03	11.3	0.
18.30	19.8	0.
18.73	20.6	196.
19.07	10.2	213.
19.60	10.2	213.
20.05	5.6	90.
20.45	0.0	0.
20.82	16.9	0.
21.18	17.8	198.
21.55	28.8	191.
21.92	28.3	186.
22.28	11.6	194.
22.63	14.1	217.
22.97	29.5	343.
23.35	28.8	191.
23.67	6.3	243.
0.05	2.8	0.
0.43	25.4	0.
1.13	26.0	168.
1.72	10.2	147.
2.07	8.9	162.
2.40	6.3	27.
2.77	12.6	64.
3.10	18.1	39.
3.40	16.5	31.
3.72	18.9	153.
4.08	18.9	153.
4.45	14.1	143.
4.75	12.6	154.
5.07	10.2	147.
5.33	10.2	147.
5.67	5.6	90.
6.40	2.8	0.
6.72	2.8	0.
7.02	4.0	315.
7.35	8.9	342.
7.68	8.5	0.
8.00	8.5	0.

TABLE A-IX

Run 4, Wind Data

TIME PDT	DIRECTION °T	SPEEDS (CM/SEC) SCALAR	EAST COMPONENT	NORTH COMPONENT
1000	147	89.4	-48.72	75.01
1100	263	89.4	88.77	10.91
1200	256	312.9	303.51	75.75
1300	283	581.1	565.99	-130.75
1400	267	402.3	401.50	20.92
1500	253	536.4	512.80	156.63
1600	244	581.1	531.13	236.51
1700	234	536.4	433.95	315.40
1800	236	581.1	481.73	324.83
1900	229	715.2	539.98	469.17
2000	232	849.3	669.25	523.17
2100	243	581.4	517.76	263.82
2200	240	491.7	425.81	245.85
2300	218	402.3	247.82	317.01
2400	270	312.9	312.9	0
0100	274	312.9	311.96	-21.90
0200	248	312.9	290.06	117.34
0300	275	491.7	489.73	-42.78
0400	288	491.7	467.61	-151.94
0500	297	357.6	318.62	-162.35
0600	301	447.0	383.08	-230.21
0700	300	268.2	232.26	-134.1
0800	307	89.4	71.43	-53.82
0900	240	178.8	154.84	89.4
1000	230	134.1	102.72	86.23
1100	230	223.5	171.20	143.71
1200	258	268.2	262.30	55.79

TABLE A-X

Run 5, GEK Data

TIME (LOCAL)	MAGNITUDE (CM/SEC)	DIRECTION (DEG TRUE)
11.80	21.5	23.
12.10	12.0	135.
12.43	16.5	121.
12.78	19.9	135.
13.13	18.1	141.
13.48	12.6	116.
13.87	5.6	0.
14.15	16.9	0.
14.50	17.1	171.
14.85	6.3	153.
15.20	6.3	153.
15.57	6.3	153.
15.92	7.9	135.
16.25	12.6	154.
16.58	11.3	0.
16.88	22.6	0.
17.25	23.3	194.
17.55	31.5	190.
17.88	31.5	190.
18.17	34.4	189.
18.53	35.7	198.
18.83	30.4	202.
19.18	32.9	211.
19.50	32.9	211.
19.90	32.9	211.
20.18	22.0	230.
20.58	24.3	234.
20.90	24.3	234.
21.25	16.5	211.
21.58	10.2	303.
21.93	6.3	27.
22.22	14.4	169.
22.55	18.1	141.
22.83	14.1	53.
23.18	14.1	53.
23.48	11.6	76.
23.83	8.9	72.
0.18	10.2	123.
0.57	12.6	116.
0.90	18.1	141.
1.25	14.4	169.
1.60	14.4	169.
2.00	15.2	158.
2.30	15.2	158.
2.62	16.5	149.
2.97	12.0	135.
3.32	8.9	162.
3.63	4.0	135.
3.98	6.3	117.
4.30	15.2	158.
4.65	15.2	158.
5.00	12.6	154.
5.32	12.6	154.
5.68	7.9	135.
6.03	5.6	0.
6.37	25.4	0.
6.75	25.4	0.
7.07	28.2	0.
7.42	28.8	191.
7.78	28.8	191.
8.17	28.8	191.

TABLE A-XI

Run 5, Wind Data

TIME PDT	DIRECTION °T	SPEEDS (CM/SEC) SCALAR	EAST COMPONENT	NORTH COMPONENT
1000	270	268.2	268.2	0
1100	242	223.5	197.35	105.05
1200	243	268.2	238.97	121.76
1300	239	312.9	268.16	161.14
1400	254	402.3	386.61	111.03
1500	261	402.3	397.47	62.76
1600	249	402.3	375.75	144.02
1700	257	402.3	391.84	90.52
1800	258	447.0	437.17	92.98
1900	248	491.7	455.81	184.39
2000	219	536.4	337.40	416.78
2100	211	491.7	253.22	421.39
2200	178	223.5	-7.82	223.28
2300	135	178.8	-126.41	126.41
2400	132	178.8	-132.85	119.62
0100	180	44.7	0	44.7
0200	202	44.7	16.76	41.44
0300	284	312.9	303.51	-75.72
0400	283	223.5	217.69	-50.29
0500	283	223.5	217.69	-50.29
0600	239	312.9	268.16	161.14
0700	296	312.9	281.30	-137.05
0800	291	312.9	292.25	-112.02
0900	282	178.8	174.87	-37.19
1000	274	223.5	223.05	-15.65
1100	280	268.2	264.18	-46.67
1200	261	312.9	309.15	48.81

BIBLIOGRAPHY

1. Bennett, D.J. and Filloux, J.H., "Magnetotelluric Deep Electrical Sounding and Resistivity," Reviews of Geophysics and Space Physics, Vol. 13, No. 3, p. 197-203, July 1975.

2. Garcia, R.A., Numerical Simulation of Currents in Monterey Bay, M.S. Thesis, Naval Postgraduate School, Monterey, 1971.

3. Hollister, J.E., Currents in Monterey Submarine Canyon, M.S. Thesis, Naval Postgraduate School, Monterey, 1975.

4. Howton, H.M., A Study of Time Variability of Surface Currents at a Point in Monterey Bay, M.S. Thesis, Naval Postgraduate School, Monterey, 1972.

5. Lipparelli, M., The GEK Signal of Lowest Mode Internal Waves, Ph.D. Thesis, Oregon State University, Corvallis, 1971.

6. Longet-Higgins, M.S., Stern, M.E., Stommel, H., The Electrical Field Induced by Ocean Currents and Waves, with Applications to the Method of Towed Electrodes, MIT and WHOI, Papers in Physical Oceanography and Meteorology, XIII(1), 1954.

7. McClelland, J.J., An Oceanographic Investigation of Thermal Changes in Monterey Bay, California, September 1971-January 1972, M.S. Thesis, Naval Postgraduate School, Monterey, 1972.

8. McKay, D.A., A Determination of Surface Currents in the Vicinity of the Monterey Submarine Canyon by the Electromagnetic Method, M.S. Thesis, Naval Postgraduate School, Monterey, 1970.

9. Pirie, D.M. and Steller, D.D., California Coast Nearshore Processes Study Final Report - ERTS-1 Experiment #088, Goddard Space Flight Center, Greenbelt, Maryland, 1974.

10. Scott, D.A., AMBAG Oceanographic Survey, Oceanographic Services, Inc., #168-2, Santa Barbara, California, p. V-7m, 1973.

11. Shepard, F.P., Marshall, N.F., and McLoughlin, P.A., "'Internal Waves' Advancing along Submarine Canyons," Science, v. 183, p. 195-198, 18 January 1974.

12. Smith, T.D., GEK Measurements of Surface Currents in Monterey Bay, 1971, M.S. Thesis, Naval Postgraduate School, Monterey, 1972.

13. Stevenson, C.D., A Study of Currents in Southern Monterey Bay, M.S. Thesis, Naval Postgraduate School, Monterey, 1964.

14. Von Arx, W.S., An Electromagnetic Method for Measuring the Velocities of Ocean Currents from a Ship Underway, MIT and WHOI, Papers in Physical Oceanography and Meteorology, XI(3), 1950.

INITIAL DISTRIBUTION LIST

	No. Copies
Department of Oceanography, Code 58 Naval Postgraduate School Monterey, CA 93940	3
Oceanographer of the Navy Hoffman II 200 Stovall Street Alexandria, VA 22332	1
Office of Naval Research Code 480 Arlington, VA 22217	1
Dr. Robert E. Stevenson Scientific Liaison Office, ONR Scripps Institution of Oceanography La Jolla, CA 92037	1
Library, Code 3330 Naval Oceanographic Office Washington, DC 20373	1
SIO Library University of California, San Diego P.O. Box 2367 La Jolla, CA 92037	1
Department of Oceanography Library University of Washington Seattle, WA 98105	1
Department of Oceanography Library Oregon State University Corvallis, OR 97331	1
Commanding Officer Fleet Numerical Weather Central Monterey, CA 93940	1
Commanding Officer Environmental Prediction Research Facility Monterey, CA 93940	1
Department of the Navy Commander, Oceanographic System, Pacific Box 1390 FPO San Francisco 96610	1

Defense Documentation Center 2
Cameron Station
Alexandria, VA 22314

Library (Code 0212) 2
Naval Postgraduate School
Monterey, CA 93940

Professor R. G. Paquette 2
Department of Oceanography
Naval Postgraduate School
Monterey, CA 93940

Associate Professor J. J. von Schwind 1
Department of Oceanography
Naval Postgraduate School
Monterey, CA 93940

W. W. Reynolds 1
Department of Oceanography
Naval Postgraduate School
Monterey, CA 93940

LT K. A. Mahumed 3
Commanding Officer
USS GALLANT (MSO-489)
FPO San Francisco, CA 96001

Apparent surface currents over the Monterey Submarine Canyon measured by the method of towed electrodes.

Thesis 162780
M27718 Mahumed
c.2
Apparent surface currents over the Monterey Submarine Canyon measured by the method of towed electrodes.